Biotechnology Advances xxx (2015) xxx–xxx

Contents lists available at ScienceDirect

Biotechnology Advances

journal homepage: www.elsevier.com/locate/biotechadv

Research review paper

Micro- and nanodevices integrated with biomolecular probes

Yunus Alapan [a], Kutay Icoz [b,*], Umut A. Gurkan [a,c,d,e,**]

[a] Case Biomanufacturing and Microfabrication Laboratory, Mechanical and Aerospace Engineering Department, Case Western Reserve University, Cleveland, OH 44106, USA
[b] Bio Micro/Nano Devices and Sensors Laboratory, Electrical and Electronics Engineering Department, Abdullah Gul University, Kayseri 38080, Turkey
[c] Biomedical Engineering Department, Case Western Reserve University, Cleveland, OH 44106, USA
[d] Department of Orthopaedics, Case Western Reserve University, Cleveland, OH 44106, USA
[e] Advanced Platform Technology Center, Louis Stokes Cleveland Veterans Affairs Medical Center, Cleveland, OH 44106, USA

ARTICLE INFO

Article history:
Received 28 April 2015
Received in revised form 6 August 2015
Accepted 5 September 2015
Available online xxxx

Keywords:
Biosensing
Micro/nanofabrication
Microcantilevers
Micro/nanopillars
Microfluidic channels
Surface functionalization
Cell adhesion
Biomolecules
Cell isolation
Point-of-care diagnosis

ABSTRACT

Understanding how biomolecules, proteins and cells interact with their surroundings and other biological entities has become the fundamental design criterion for most biomedical micro- and nanodevices. Advances in biology, medicine, and nanofabrication technologies complement each other and allow us to engineer new tools based on biomolecules utilized as probes. Engineered micro/nanosystems and biomolecules in nature have remarkably robust compatibility in terms of function, size, and physical properties. This article presents the state of the art in micro- and nanoscale devices designed and fabricated with biomolecular probes as their vital constituents. General design and fabrication concepts are presented and three major platform technologies are highlighted: microcantilevers, micro/nanopillars, and microfluidics. Overview of each technology, typical fabrication details, and application areas are presented by emphasizing significant achievements, current challenges, and future opportunities.

Contents

* Corresponding author.
** Correspondence to: U.A. Gurkan, Glennan Building, Room 616B, 10900 Euclid Ave., Cleveland, OH 44106, USA.
E-mail addresses: kutay.icoz@agu.edu.tr (K. Icoz), umut@case.edu, http://www.case-bml.net (U.A. Gurkan).

http://dx.doi.org/10.1016/j.biotechadv.2015.09.001
0734-9750/

1. Introduction

Detection and analysis of biomolecules for medical diagnostics, environmental monitoring, and quality control of food products have always drawn great attention and been an active topic of research due to their direct impact on human life. For instance, detection of cancer biomarkers or circulating tumor cells (CTCs) in patient blood would allow early diagnosis and timely intervention of the disease (Adams et al., 2008; Nagrath et al., 2007; Stott et al., 2010). Similarly, detection of airborne pathogens can lead to early counter measures (Lee et al., 2008a; Meltzer et al., 2011). Moreover, food analysis for quality and safety control is critical for production and supply chain in today's world (Atalay et al., 2011; Crevillen et al., 2007). Collaboration of various engineering and science disciplines under the canopy of nanotechnology has brought together innovative methods and techniques enabling revolutionary micro/nanodevices that can identify and recognize nucleic acids, proteins, viruses, bacteria, and cells.

Biological molecules utilized to detect and/or monitor amount and activity of proteins, nucleic acids and cells are called biomolecular probes. In the human body, biomolecules are present either in a soluble form, such as the proteins in the blood (Adkins et al., 2002; Schmid et al., 1956), or they are an integral part of a cell, such as the cell membrane surface antigens and receptors (Aplin et al., 1998; Pierce et al., 2002; Wang et al., 2012). Receptor–ligand interactions are essential components of the structural and functional complexity found in the living organisms (Cozens-Roberts et al., 1990; Hynes, 1999). Mimicking nature, biomolecular probes have been the key component of many recent biomedical micro/nanodetection systems and biosensors. Here, we use the term "biosensor" as a general expression for biomicro/nanodetection and analysis tools.

In general, biosensors are composed of three main parts: (1) probe (detector), (2) transducer, and (3) signal processor (Fig. 1). Specific biological recognition is generally accomplished by the biomolecular probe (e.g., receptor, ligand, antibody, aptamer, extracellular matrix proteins). Then, the transducer converts biomolecular recognition events into measurable signals. Transducer output signal can be optical, electrochemical, electrical, thermal, magnetic, mechanical, or a combination of these based on the system design (Collings and Caruso, 1997; Gooding, 2002; Paddle, 1996). Finally, the processing unit (e.g., microprocessor) filters, amplifies, analyzes, and displays the output signal or result. Advances in semiconductor technology enabled producing not only silicon-based electronic circuits, but also electromechanical devices made of polymers, metals, carbon, and silicon, commonly referred to as microelectromechanical systems (MEMS) and nanoelectromechanical systems (NEMS) (Grayson et al., 2004; Moore and Syms, 1999; Staples et al., 2006). Various transducers have been developed using the MEMS and NEMS biosensor technologies, including cantilevers, pillars, microfluidics, nanopores, carbon nanotubes (CNTs), nanoparticles, and nanowires (Gao et al., 2007; Howorka et al., 2001; Inci et al., 2013b; Moon et al., 2011; Raiteri et al., 2001; Tan et al., 2003). Performance of these micro/nanodevices highly depends on biomolecules immobilized on the device as probes, which is discussed in this review.

2. Biomolecular probes

Interactions between biomolecules and the biosensors constitute a critical component for the design of novel and efficient biosensing approaches. Therefore, understanding the physicochemical, biochemical, and biophysical characteristics of biomolecular probes is important in

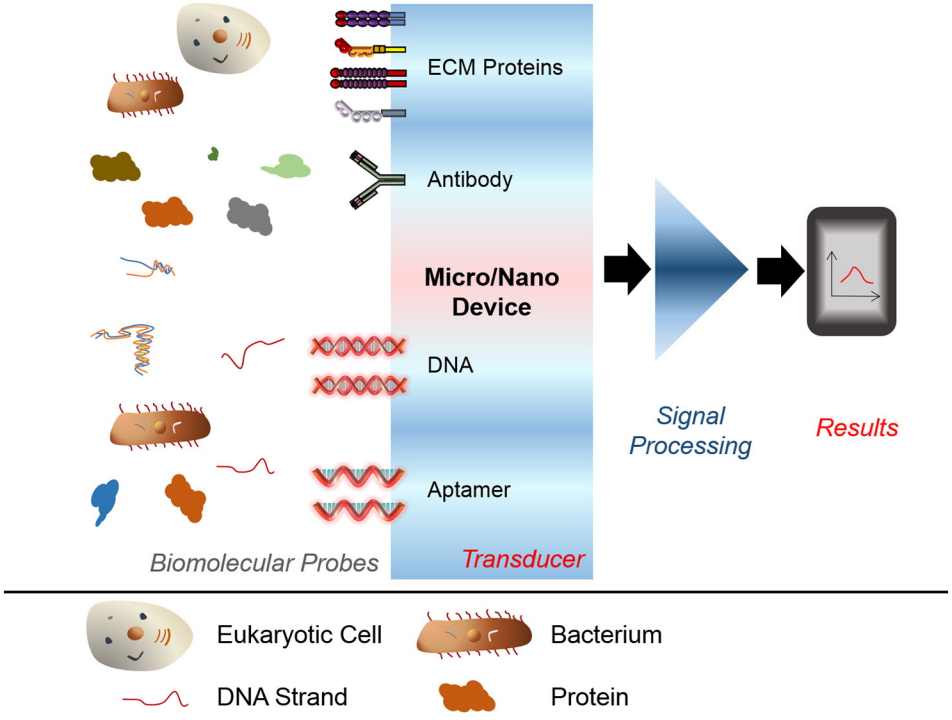

Fig. 1. Schematic representation of a biosensor and essential components. Biomolecular probes include antibody, DNA, aptamer, and extracellular matrix (ECM) proteins. Using micro/nanobiosensors, nucleic acids, proteins, bacteria, and cells can be detected, their amount can be measured and their activity can be analyzed based on interactions occurring through biomolecular probes immobilized on the transducer surface. Transducers convert biological signals into measurable signals which are processed and analyzed.

Please cite this article as: Alapan, Y., et al., Micro- and nanodevices integrated with biomolecular probes, Biotechnol Adv (2015), http://dx.doi.org/10.1016/j.biotechadv.2015.09.001

micro/nanodevice design and development (Folch, 2012). Adhesion of a molecule to a surface is known as adsorption. If adsorption is governed solely by physical forces, it is called physisorption. On the other hand, if adsorption is mediated by chemical interactions between a surface and a molecule, then it is called chemisorption. Physical interactions playing a role in biomolecular probe–device surface interactions can be grouped under four major categories: (i) van der Waals forces, (ii) hydration forces, (iii) hydrogen bonds, and (iv) hydrophobic forces. Physisorption processes do not necessitate special treatments, such as surface activation via ozone treatment and chemistry expertise (including covalent binding of biomolecules to the surface via cross-linkers and proteins) compared to the chemisorption procedures. On the other hand, physisorbed coatings are regarded as unstable in terms of their adhesion to the adsorption surface in comparison to chemisorbed coatings (Folch, 2012).

Cell adhesion, mediated by a variety of biomolecules, plays a critical role in vital cellular processes, including proliferation, survival, and gene expression (Cozens-Roberts et al., 1990; Hynes, 1999). Biomolecules of cellular adhesion can be categorized into four main groups (Fig. 2): (i) immunoglobulins, (ii) selectins, (iii) cadherins, and (iv) integrins (Hynes, 1999). Immunoglobulin superfamily is primarily involved in the immune system for marking unwanted cells, bacteria and viruses, and they exhibit a significant specificity which is critical for recognizing and counteracting foreign bodies. Selectins play an important role in normal as well as abnormal white blood cell (WBC) adhesion to the endothelium (Springer, 1990). Cadherins are important in cell–cell adhesion, such as in the formation of a uniform endothelium by endothelial cells that covers the lumens of blood vessels (Angst et al., 2001). Integrins are mainly associated with cell–extracellular matrix (ECM) interactions and adhesion, such as in the modulation of cell migration on ECM by the formation of new bonds in the direction of movement and disruption of the older ones in the opposite direction (Huttenlocher and Horwitz, 2011; Hynes, 1999). Immunoglobulins and selectins are mainly involved in adhesion initiation and early stage binding of cells (Leckband et al., 2000; Mehta et al., 1998).

Immunoglobulins, also known as antibodies, bind to specific parts of a foreign object, namely the antigen, and they can be immobilized on biosensor components or surfaces. Antibodies significantly enhance the detection limit and performance of biosensors due to their extremely high specificity and high binding constants of 10^{9}–10^{12}. Using antibodies, biomolecule concentrations as low as in the picomolar range (10^{-12} M) can be analyzed (Lowe et al., 1990). Because of their high selectivity and binding interactions, antibodies are commonly utilized in biosensor applications (Collings and Caruso, 1997; El-Sayed et al., 2005; Inci et al., 2013a,b; Raiteri et al., 2001).

Aptamers are artificial oligonucleotides, which may be of single stranded DNA/RNA or peptide origin (Cho et al., 2009). Aptamers are designed to have a specific structural conformation that provides binding to target entities or to change structure upon target interaction (Nutiu and Li, 2003). Aptamers have specific advantages over antibodies: (i) once the sequence is determined, aptamer synthesis is relatively easy and custom manufacturing is possible, (ii) aptamers can be reversibly denatured, for controlled binding and release of target molecules (Shastri et al., 2015), and iii) aptamers include phosphodiester bonds which are chemically stable. Due to these advantages, aptamers have been used as biomolecular probes in a number of biosensing platforms in combination with: cantilevers (Savran et al., 2004), optical diffraction biosensors (Lee et al., 2010), surface plasmon resonance biosensors (Cho et al., 2012; Lee et al., 2008b), nanotubes (So et al., 2005), and microfluidic devices (Sheng et al., 2012), to detect various biomolecules, such as PDGF-BB (Lee et al., 2010), leukemia cells (Sheng et al., 2012), and bacteria and viruses (Hong et al., 2012). Antibodies are not affected by nucleases and have been well developed for many years. To benefit from the advantages of both antibodies and aptamers, hybrid systems have been developed (Ohk et al., 2010; Zhang et al., 2014). Fiber-optic sensor (Ohk et al., 2010) and microfluidic systems (Zhang et al., 2014) incorporating immobilized antibodies and aptamers on the same surface as recognition molecules demonstrate higher capture efficiency compared to antibody alone or aptamer alone designs.

Technical needs in diagnostic medicine for quantifying clinically meaningful cell–biomolecule interactions in healthy and diseased states paved the way for the development of various micro/nanotechnologies, such as point-of-care $CD4^{+}$ T-cell microchip for HIV patient monitoring (Gurkan et al., 2011a; Moon et al., 2011; Wang et al., 2014; Shafiee et al., 2015; Unal et al., 2014; Gurkan et al., 2011b), $CD34^{+}$ endothelial progenitor cell microchips for cardiovascular medicine (Hansmann et al., 2011; Hatch et al., 2011), sickle cell disease (SCD) monitoring biochip (Alapan et al., 2014), and CTC chips for cancer (Nagrath et al., 2007; Stott et al., 2010). These micro/nanotechnologies have been tested and proven to be effective with diseases that have a significant socioeconomical impact affecting millions of people worldwide.

For example, SCD is estimated to affect more than 100,000 Americans and 5 million Africans, causing painful crisis, widespread organ damage, and early mortality (Hassell, 2010; Makani et al., 2011). One of the most prominent signs of SCD is the vaso-occlusive crisis, which is caused by selectin mediated abnormal adhesion of WBCs, and BCAM/LU mediated abnormal adhesion of sickled red blood cells (RBCs) to vascular endothelium (Alapan et al., 2014; Barabino et al., 1987a,b, Chang et al., 2008; Hebbel et al., 1980, 1981). Similarly, cell adhesion plays an important role in the progression of cancer and metastatic dissemination of tumor cells (Cavallaro and Christofori, 2004; Rizvi et al., 2013). Fundamental insight into cell adhesion mediated by biomolecules would enable in-depth investigation of disease progression and allow the development of novel therapeutics and sensing technologies. Furthermore,

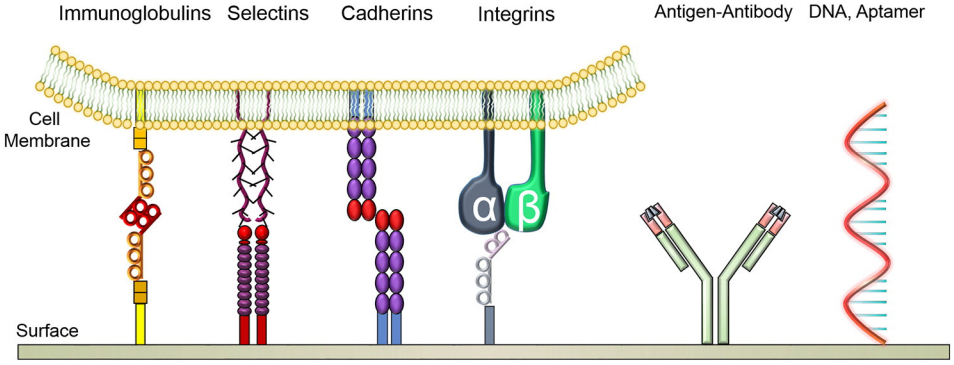

Fig. 2. Four major categories of receptors on cell membrane playing role in cellular adhesion, and antibody, DNA, aptamer strands as biomolecular probes. Immunoglobulins (Igs, antibodies) are primarily associated with immune system, whereas selectins are involved in white blood cell homing. Immunoglobulins and selectins show high affinities with rapid binding rates. Cadherins and integrins are mainly involved in cell–cell and cell–matrix interactions, respectively. DNA and aptamer strands have been used as biomolecular probes with high specificity.

Please cite this article as: Alapan, Y., et al., Micro- and nanodevices integrated with biomolecular probes, Biotechnol Adv (2015), http://dx.doi.org/10.1016/j.biotechadv.2015.09.001

cell–biomolecule interactions and adhesion have vast implications in fundamental biological processes including cellular differentiation (Li et al., 2012; Wang and Chen, 2013), mitosis (den Elzen et al., 2009; Suzuki and Takahashi, 2003), motility and migration (Gardel et al., 2010; Maheshwari et al., 2000), and cell homing (Jin et al., 2006; Vermeulen et al., 1998). Therefore, micro/nanotechnologies that take advantage of these vital biological interactions open new venues and allow new analyses in biology and medicine (Tasoglu et al., 2013).

In the next sections, we focus on three promising micro- and nanoscale systems that are utilized for mainstream biosensing applications in cellular biology and clinical medicine: microcantilevers, micro/nanopillars, and microfluidics. These systems have been developed to investigate bimolecular detection and cellular interactions. We introduce these systems, describe design/fabrication steps for a typical device in each category, and review applications of these systems in biology and medicine.

3. Microcantilevers

Micro/nanocantilevers have been designed and used as label-free biosensors (Figs. 3 & 4). Cantilevers convert biological signals into mechanical deflections that can be detected using optical, electrical and magnetic methods (Fritz et al., 2000; Gupta et al., 2004a; Ilic et al., 2000; Johnson et al., 2006; Li et al., 2006; Sone et al., 2006; Wu et al., 2001). Cantilever operation can be classified into two groups: static mode and resonant mode. In static mode operation, biomolecular interactions on cantilever surface cause deflection of the free end of the cantilever (Fig. 3a & b). In resonant mode operation, biological mass, such as a cell, changes the vibration frequency of the cantilever. Next, the change in vibration frequency can be measured by optical means to quantify the mass. Cantilevers are generally fabricated from silicon, silicon oxide, or silicon nitride. Today, fabrication of cantilevers using these semiconductor materials is a standard cleanroom process (Fig. 4a). Polymer-based cantilevers for biosensing applications have also been reported. Fluorocarbon coated polymeric cantilevers have been shown to offer advantages over gold coated silicon nitride cantilevers, such as stability against temperature and pH changes (Calleja et al., 2006). Numerous biosensor systems based on surface functionalized cantilevers have been implemented with biomolecular probes for the detection of various biological targets, such as kinases and myoglobins (Arntz et al., 2003), glucose (Pei et al., 2004), bacterial cells, including *Escherichia coli* (Ilic et al., 2000), *Listeria innocua* (Gupta et al., 2004a), *Bacillus subtilis* spores (Dhayal et al., 2006), vaccinia virus particles (Johnson et al., 2006), RNA (Zhang et al., 2006), and cancer markers (Wu et al., 2001).

3.1. Fabrication and functionalization of microcantilevers

In this section, fabrication process of silicon nitride cantilevers is described as a case study. In a typical case, 4-inch diameter, 500 μm thick, single-side polished, silicon wafers are used as the bulk material. The fabrication process starts with a standard RCA cleaning. The silicon wafer is then coated with 0.5 μm low stress (silicon-rich) silicon nitride to form cantilevers by low-pressure chemical vapor deposition (LPCVD). Cantilever material (low stress silicon nitride) is patterned through two photolithography and plasma etching steps (Fig. 4a). Each photolithography step includes 2-μm-thick positive photoresist spinning, pre-baking at 100 °C for 1 min, ultraviolet (UV) light exposure for 8 s, wet resist development for 10 s, and post-baking at 120 °C for 2 min. Cantilevers are defined by front side photolithography on the polished side of the silicon wafer, followed by a plasma etch of the nitride. Photoresist layer is not removed and kept on the front surface as a protection layer during the second plasma etch of the back side. Dies are defined on the unpolished side (back side) of the silicon wafer by photolithography using the front side for alignment. Both the nitride layers on the front and back sides serve as an etch mask for wet etching of the bulk silicon in potassium hydroxide. After the photolithography step, back side nitride is etched by a plasma etch again. The photoresist layers on both sides of the wafer are cleaned using piranha solution and solvent cleaners. Finally, the devices are released with a wet etch of the bulk silicon in 45% potassium hydroxide solution at 80 °C over a period of 7 h (Fig. 4b) (Icoz and Savran, 2010).

After fabrication, the cantilever needs to be coated (usually by metals, such as gold). This coating enables chemical functionalization of the cantilever and provides a highly reflective surface for the laser light, which is used to detect the deflection of the cantilever. Usually, gold coating is used, because the alkane chain with thiol groups bind to gold covalently (Raiteri et al., 2001; Storri et al., 1998), which allows custom surface functionalization for many different applications. Cantilevers are functionalized using various methods such as dimension-matched capillaries (Bietsch et al., 2004; Savran et al., 2002), pipetting droplets, spray-coating (Battiston et al., 2001), and inkjet printing (Bietsch et al., 2004). Among these methods, inkjet printing (nanojet dispensing) has advantages, such as easy droplet generation and spatial accuracy. Inkjet printing enables separate functionalization of differential cantilever arms so that each arm can be coated with different biomolecules.

3.1.1. Cantilever operation modes: static versus resonant

In the static mode, the adsorption of molecules onto the surface generates a 'surface stress' that causes the cantilever to bend slowly, which

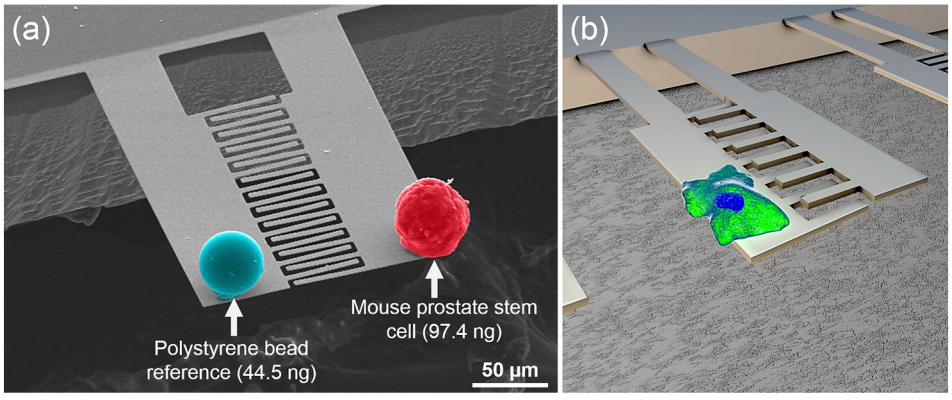

Fig. 3. Probing cellular weight on microcantilevers. (a) A polystyrene bead is placed on the control arm and a stem cell is placed on the sensing arm. Double resonance frequencies are quantified in a single measurement. In this example, the mass of the polystyrene bead was measured as 44.5 ng and the mass of the mouse stem cell was measured as 97.4 ng. For details see Chan et al. (2013, 2014). (b) Illustration of a cell adhered and spread on a microscale cantilever for cell detection and/or cellular mass measurement. The weight of the cell is sufficient to deflect microcantilevers and change their resonant frequency. This approach exploits differences in resonance frequency shift of the microcantilever after cell attachment and growth, since system frequency is reversely correlated with mass.

Please cite this article as: Alapan, Y., et al., Micro- and nanodevices integrated with biomolecular probes, Biotechnol Adv (2015), http://dx.doi.org/10.1016/j.biotechadv.2015.09.001

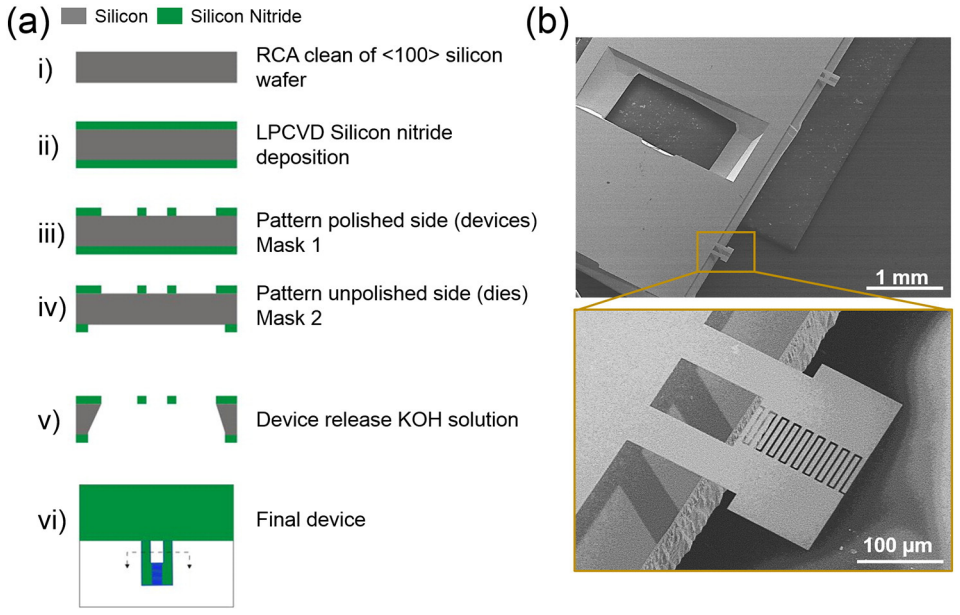

Fig. 4. Production of a typical microcantilever by using photolithography and plasma etching. (a) Fabrication process of differential silicon nitride (SiNi) cantilevers. Only major steps are shown: (i–v) Cross-sectional view, (vi) top view. (b) Scanning electron micrographs of the die and differential nanomechanical biosensors. Inset shows a higher magnification image of an individual differential nanomechanical biosensor.

is why this mode is commonly referred as 'static' bending. Usually, a laser beam is focused on the tip of the cantilever and the reflected beam is detected by the optical lever method using split photo detectors that can measure the deflections with high accuracy (0.1 nm accuracy has been reported for this method (Fritz et al., 2000)). The well-known Stoney's equation (Stoney, 1909) explains the relation between the surface stress change and cantilever's tip deflection:

$$\Delta z = 3\frac{(1-\nu)}{E}\frac{L^2}{t^2}\Delta\sigma \quad , \tag{1}$$

where Δz is cantilever's tip deflection, ν is Poisson' ratio, E is Young's modulus, L is the length of the cantilever, t is the thickness of the cantilever, and $\Delta\sigma$ is the change in surface stress (N/m). Gold coated silicon cantilever arrays were used by Fritz et al. to the detect mismatch of oligonucleotides, which is considered as a pioneering work in the field (Fritz et al., 2000). Arrays of individually functionalized cantilevers have been employed for label-free detection of multiple DNA strands (McKendry et al., 2002). These studies were reported more than a decade ago, and since then, gold coating has widely been adopted as a preferred method of covalent thiol-based probe immobilization.

The resonant mode, in essence, is 'mass' detection. When the cantilever is loaded with additional mass, resonant frequency decreases and the additional mass can be calculated by:

$$\Delta m = \frac{k}{4\pi^2}\left(\frac{1}{f_1^2}-\frac{1}{f_0^2}\right), \tag{2}$$

where k is the spring constant, f_0 is the initial frequency, and f_1 is the resonant frequency after the mass loading. In order to increase sensitivity, external actuation through piezoelectric devices may be used to create vibrations at specific frequencies (Johnson et al., 2006). Gupta et al. used silicon cantilevers in resonant mode for biosensing (Gupta et al., 2004a). The resonant frequencies of unloaded and loaded cantilever with *L. innocua* cells (Gupta et al., 2004a) and virus particles (Gupta et al., 2004b) were measured, in which Eq. (2) was employed to calculate the mass of a single virus particle.

3.2. Applications of microcantilevers

Cantilever transducers have been extensively developed for chemical and biological sensing. Even though the standard structure of a cantilever is similar to a diving board, where one end is fixed and the other end is free, various geometric changes are possible to meet the signal transduction requirements and surface biochemical reactions (Figs. 3 & 4). Interferometric cantilevers are differential transducers that are composed of two beam structures and interdigitated fingers between them (Fig. 3). They were first developed for Atomic Force Microscopy (AFM), in which cantilevers were used as scanning probes (Manalis et al., 1996; Onaran et al., 2006; Yaralioglu et al., 1998). Particularly due to the advantages of interferometric cantilevers in AFM applications, the same methods have been applied to biosensors (Savran et al., 2002; Sulchek et al., 2001). In such an application, aptamer molecules can be immobilized on the gold-coated sensor surface with a thiol linker (Savran et al., 2004). Single-stranded DNAs (ssDNAs) are immobilized onto the reference cantilever in order to prevent nonspecific binding. The L-shaped geometry of the sensor allows each cantilever to be functionalized individually by dipping one side (either the sensor part or the reference part) into a micropipette. In this arrangement, ligand–aptamer binding creates a surface stress change which bends the sensor cantilever, while the reference cantilever remains unaffected. The tip deflection of the cantilever is measured using a laser beam based on interferometry differential measurements, which has considerable advantages over single measurements in terms of background noise (Bronzino, 2000). Cantilever structures that have two layers can be used as temperature sensors with a sensitivity of 2 μK. This method is based on the different thermal expansion coefficients of the layer materials (Lai et al., 1997). However, differential measurement minimizes this unwanted effect. This result was demonstrated by recording the absolute deflection and the differential deflection of the cantilevers in response to temperature change. Researchers who do not use differential cantilevers employ other methods to reduce noise. For instance, Fritz et al. employed one cantilever as a control and used optical lever measurements twice to subtract background noise from the biological signal (Fritz et al., 2000). In another case, Alvarez and Tamayo employed a scanning laser source for recording measurements from cantilever arrays (Alvarez and Tamayo, 2005). Both of

these techniques required additional signal processing and more complex measurement systems when compared with the interferometric cantilevers (Alvarez and Tamayo, 2005; Fritz et al., 2000; Sulchek et al., 2001).

Another novel cantilever design is presented in (Burg et al., 2007). A microfluidic channel was produced on the top surface of a silicon cantilever to flow the biomolecules over the free-end of the cantilever. Resonant frequency shifts upon the loading of molecules in the microfluidic channel were detected. This cantilever was able to weigh single nanoparticles and single cells such as *E. coli* and *B. subtilis*. Even though fabricating microchannel adds complexity to the fabrication process, one of the biggest advantages of such systems is the ease of surface functionalization, which is accomplished by just maintaining fluid flow in the microchannel.

Magnetic beads functionalized with biomolecules may be used with cantilevers to improve sensitivity and selectivity. Magnetic beads can be separated from complex environments by applying external magnetic fields. A demonstration of the employment of magnetic beads with cantilevers for a biosensor application has been performed (Weizmann et al., 2004), where viral DNA detection of M13phi was successfully reported at extremely low concentrations, as little as 7.1×10^{-20} M. Recently, actuation of cantilevers at a low noise region using magnetic beads was also presented. In such a report, the control arm of the differential cantilever was passivated with bovine serum albumin (BSA) and the sensing arm was probed with biotin-BSA using a nanojet dispensing system (Icoz et al., 2008; Icoz and Savran, 2010). It was observed that the streptavidin coated magnetic beads were mostly bound to the sensing arm and the applied external magnetic field caused relative deflection of cantilevers. The electromagnet was controlled by a function generator so that the frequency of the excitation signal could be adjusted. This way, cantilevers were excited at a low noise region allowing a deflection resolution of as little as 0.065 Å.

Galbraith and Sheetz measured the traction forces of fibroblast cells during migration by utilizing flexible horizontal cantilevers (Galbraith and Sheetz, 1997). The MEMS device used in this study incorporated mounted horizontal cantilevers and pads, where cell–biomolecular probe interactions occurred at the tip of these cantilevers. By imaging the deflection of the cantilevers, traction forces were calculated during locomotion of the cells. Limitation of this MEMS device is the measurement of forces projected along only one axis.

Mass of single cells can be measured in fluid (Park et al., 2008) or in air (Chan et al., 2013) by using cantilevers. In a fluidic state, He-La cells were attached to cantilever arrays coated with poly-L-lysin as a biomolecular probe and dielectrophoresis was used to capture the cells in fluid flow. Cells were cultured on the cantilever surface and the resonance frequency changes were measured by a laser Doppler vibrometer to quantify the mass of each cell (Park et al., 2008). In air, stem cells, spore clusters and diatoms were first specifically selected from an environment including many cells with a micromanipulator and then placed on a differential cantilever for measurement. Double resonance frequencies (two resonance frequencies from two cantilever arms) were observed in a single measurement and the mass of each cell was calculated using the frequency shifts (Fig. 4) (Chan et al., 2013). This system combines the micromanipulator and the microcantilever by taking advantage of both systems in terms of selectivity and differential measurement.

4. Micro/nanopillars

Micro/nanopillars are vertically utilized adaptations of horizontal cantilevers (Fig. 5a & b) providing a 2D semi-continuous substrate for adhesion of cells (Fig. 5c). Pillars can be functionalized with a variety of biomolecular probes for various applications. For example, cells can attach, spread, and migrate on pillar surfaces by applying traction forces through their attachment sites to the pillar surface. This traction force results in the deflection of the pillar, which behaves as an elastic spring that is governed by the simple force–deflection equation:

$$F = \left(\frac{3EI}{L^3}\right)\delta \ , \tag{3}$$

where F is the force, E is Young's modulus, I is the moment of inertia, L is the length, and δ is the deflection of the pillar. Cell traction forces can be calculated by imaging the pillar deflection using a microscope and an image correlation algorithm. Here, fabrication of pillars at the micro- and nanoscale is discussed and their applications in biology are presented.

4.1. Fabrication and functionalization of micro/nanopillars

Fabrication of pillar structures at the micro- and nanoscale is an integral and challenging component of pillar substrates. Even though there are relatively simple methods to fabricate pillars at the microscale, advanced manufacturing techniques are utilized to produce pillar arrays

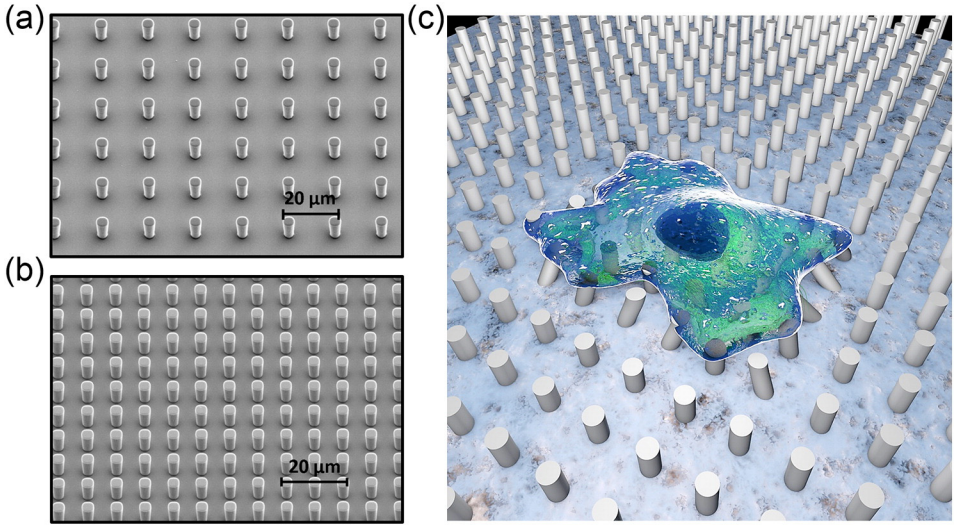

Fig. 5. Micropillar substrates can be modified to change topographical environment of cells. (a, b) SEM images of micropillar substrates with different array configurations and dimensions. Change in micropillar size, height, and spacing affects topographical cues for the cells, which has implications in cell spreading, alignment, migration, and differentiation. (c) Depiction of a single cell adhered on microscale pillar structures via biomolecules on cell membrane. When cells attach, spread, and migrate on a substrate they apply traction forces to the substrate, which in this case results in deflection of micropillars and, thus enables calculation of traction forces.

Please cite this article as: Alapan, Y., et al., Micro- and nanodevices integrated with biomolecular probes, Biotechnol Adv (2015), http://dx.doi.org/10.1016/j.biotechadv.2015.09.001

with high spatial density and aspect ratio, or pillar structures with nanoscale dimensions.

4.1.1. Microscale pillar fabrication and functionalization

Replica molding has been the gold standard for micropillar array fabrication in the literature. In replica molding, a prepolymer is cast in a template with the desired geometry and dimensions, and the pillar array is peeled off from the template after curing. Even though basic principles of the replica-molding protocols are similar in published literature, there are various techniques to fabricate pillar templates. Standard photolithography (also known as contact photolithography) and chemical developing processes allow fabrication of micropillar array templates with low spatial densities and smaller aspect ratios (≈1:5). On the other hand, for micropillar array templates with high spatial densities and high aspect ratios (>1:5), stepper photolithography (also known as projection photolithography) and deep etching processes are utilized (Yang et al., 2011).

Standard replica molding procedure was applied by numerous studies in the literature for fabrication of micropillars with dimensions ranging from 2 to 10 μm in diameter, 3 μm to 50 μm in height, and with 9 μm spacing (Lemmon et al., 2005; Sniadecki et al., 2007; Tan et al., 2003; Ting et al., 2012). Briefly, a positive SU-8 template on a silicon wafer consisting of an array of holes was obtained by using photolithography to fabricate an array of pillars. Subsequently, a prepolymer of poly(dimethylsiloxane) (PDMS) was poured over SU-8 pillars, cured, and peeled off resulting in a negative template. The negative template was oxidized in air plasma, and silanized ((Tridecafluoro-1,1,2,2-Tetrahydrooctyl)-1-Trichlorosilane) under vacuum to facilitate an easy separation of PDMS. Afterwards, micropillars were produced by molding prepolymer of PDMS into the negative template, degassing under vacuum, curing and peeling off from the template. Fig. 6a depicts the schematic of a typical replica-molding process. Furthermore, the tips of the micropillars can be functionalized by microcontact printing via premade PDMS stamps that were immersed in ECM proteins (Fig. 6b).

The replica molding process was also utilized to obtain high spatial density micropillars with dimensions of 1 μm to 2 μm in diameter, 3 μm to 8 μm in height, and from 2 μm to 4 μm spacing (du Roure et al., 2005; Rabodzey et al., 2008). In these studies, photolithography was used to produce the negative template with the desired hole pattern and depth on silicon wafers, followed by a deep etching process (Bosch Process) for increased spatial density. After silanization of the negative template, PDMS was molded, cured and peeled off, resulting in micropillar arrays. Afterwards, micropillars were oxidized and sterilized in air plasma to enhance adsorption of biomolecular probes, such as fibronectin.

To improve the versatility of micropillar substrates by including a force actuation capability, Sniadecki et al. embedded nanowires (diameter: 305 nm, length: 5–7 μm) into PDMS pillars (diameter: 3 μm, length: 10 μm) (Sniadecki et al., 2007). Nanowires were embedded into PDMS pillars by employing the following steps: (i) placement of nanowires in the pillar template, (ii) vertical alignment of nanowires through magnets placed under the templates, and (iii) molding PDMS into the templates after nanowire settlement.

Ghassemi et al. manufactured pillar structures with varying height and uniform top surface topology in the same array (Ghassemi et al., 2008). Micropillar dimensions were ranged from 0.7 μm to 3 μm in

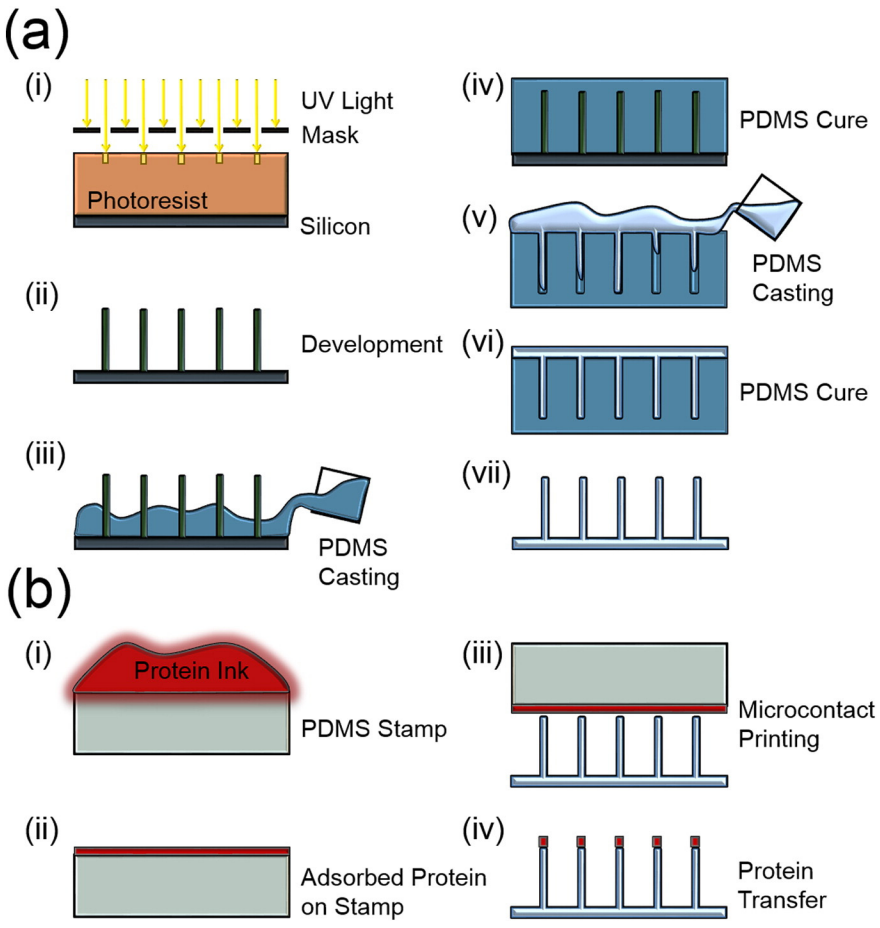

Fig. 6. Fabrication and surface modification of micropillar substrates. (a) Micropillar fabrication: (i) Pattern formation on photoresist material (SU-8) through photolithography using a photomask, (ii) development of photoresist via wet etching, (iii) PDMS casting, (iv) PDMS cure, (v) second PDMS casting, (vi) second PDMS cure, and (vii) final pillar substrate. (b) Schematic drawing of surface modification: (i) Incubation of protein on a PDMS block, (ii) protein adsorption on stamp, and (iii) and (iv) microcontact printing for protein transfer to micropillar top surfaces.

Please cite this article as: Alapan, Y., et al., Micro- and nanodevices integrated with biomolecular probes, Biotechnol Adv (2015), http://dx.doi.org/10.1016/j.biotechadv.2015.09.001

diameter and 2 μm to 8 μm in height. First an array of holes were formed with uniform heights on a silicon wafer surface by using photolithography and reactive ion etching. To fabricate a stepped array of micropillars, first, silicon dioxide was deposited with a thickness of 2 μm over the entire wafer. Afterwards, another photolithography and etching step was applied to finish the forming of the template. Finally, after cleaning and silanization processes, PDMS was molded into template to produce the micropillar substrate with varying height and uniform topology. In a follow-up study, Ghassemi et al. fabricated gold-tipped micropillars to allow different surface chemistries (Ghassemi et al., 2009). By utilizing the same technique (Ghassemi et al., 2008), a template with a uniform height was made and deposited with chromium with a 30° angle via an electron beam evaporator while rotating the template. Using this method, a chromium layer was formed on the top and upper lateral parts of the pillars. Then, a 20 nm layer of gold was deposited, followed by 5 nm titanium deposition via an electron beam evaporator at a normal angle, where the chromium layer on top of the pillars prevented the gold deposition on the sidewalls of the pillars. After removal of the sacrificial chromium layer, PDMS was molded into the template and micropillar arrays with gold tips were peeled off.

4.1.2. Nanoscale pillar fabrication and functionalization

Even though there are studies in the literature which push the limits of top-down fabrication, it is inherently difficult to fabricate pillar structures at the nanoscale, especially with dimensions smaller than 100 nm. Therefore, researchers have adapted hybrid approaches to fabricate nanopillar arrays.

Bucaro et al. fabricated nanopillars ranging from 100 nm to 750 nm in radius, 5 to 10 μm in height and 0.8 to 5 μm in spacing (Bucaro et al., 2012). In this approach, deep UV stepper lithography and deep reactive ion etching were utilized to make the silicon template. Then, double molding was applied, to first obtain the negative PDMS replica and then the positive PDMS replica of the template.

Hu et al. fabricated nanopillars with dimensions ranging from 150 nm to 1 μm in height, 40 nm to 80 nm in diameter, and 100 nm pitch by using nanoimprinting with in situ elongation (Hu et al., 2010). First, a silicon mold with 100 nm spacing, 80 nm diameter, and 500 nm deep pores was obtained via plasma etching. When the mold was filled with polystyrene at 150 °C, adhesion forces between polystyrene and silicon on pillar top surfaces during the vertical withdrawal of the mold caused an axial tension. This tension caused the elongation of the pillars at temperatures where polystyrene was still soft. As a result, pillar diameter decreased with increasing pillar elongation due to volume conservation, which resulted in nanoscale pillar structures.

Kuo et al. utilized nanosphere lithography and nanomolding to fabricate nanopillars with dimensions ranging from 100 nm to 380 nm in diameter, 600 nm to 1 μm in height with 400 nm spacing (Kuo et al., 2010, 2011). Close-packed polystyrene nanospheres were grown on a silicon substrate by spin coating. Sizes of the nanospheres were regulated by trimming the nanospheres via oxygen plasma etching for the desired diameter of the template. Then, an electron beam evaporator was used to deposit a nickel layer on polystyrene beads. Afterwards, polystyrene beads were removed via sonication in dichloromethane and acetone solution. The remaining nickel on the silicon substrate was used as an etch mask for the induced coupled plasma etching process with tetrafluoromethane and argon gasses. After fabrication of the template is completed, SU-8 photoresist was spun on the template, vacuumed to prevent air bubbles, exposed to UV radiation, baked, and then peeled off from the template to obtain nanopillars. Green fluorescent quantum dots were mixed with SU-8 before molding to label SU-8 nanopillars with green fluorescence.

4.2. Applications of micro/nanopillars

Cells, in their native environment, are in contact with topographies ranging from macro- to micro- and nanoscale dimensions. Macroscale topographies are reflected in organ and tissue level architecture (i.e., bone, blood vessel, and tendon), microscale topographies are present in cellular level architecture (i.e., organization and morphology of neighboring cells), and nanoscale topographies are reflected in subcellular architecture (i.e., protein conformations). Cellular interactions with all of these topographies at different dimension scales affect cell behavior and function (Griffin et al., 2015; Kshitiz et al., 2012; McNamara et al., 2010). Microscale features are in the same order of scale with cells, resulting in alignment and organization of cells in tandem with these features (Griffin et al., 2015; McNamara et al., 2010). However, nanoscale features are three orders of magnitude smaller than of cells, corresponding to the size scale of cellular proteins, such as the cell membrane receptors. Even though micropillars can be utilized as a surrogate for controlling microscale environment of cells, pillar structures at the nanoscale enable studies of cellular behavior at the molecular scale.

Pillar arrays have been adapted for the study of a diverse set of problems in cellular biology (Fig. 7) due to their inherently simple structure, easy modification of physical properties and accurate sensing of cellular forces (Sniadecki et al., 2006; Unal et al., 2014). Most of the studies incorporating micro- and nanoscale pillar substrates were focused on analysis of the cell adhesion process, specifically the generated traction forces at adhesion sites, and their effects on cell behavior, such as morphology, migration, and differentiation (Ghibaudo et al., 2008; Saez et al., 2007; Yang et al., 2011). Cell traction forces have been shown to be a critical determinant in various physiological and pathophysiological events, including angiogenesis, inflammation, and metastasis (du Roure et al., 2005; Kraning-Rush et al., 2012; Wang and Li, 2009). Understanding the relationships between generated traction forces and cellular behavior can reveal the mechanisms of these events at the cellular and sub-cellular levels. Pillar substrates can be utilized for the measurement of cellular traction forces in various applications and as a controlled environment to study cell–ECM interactions (Table 1). Furthermore, pillar arrays can be used as an active structure to apply external physical cues, such as electrical, mechanical, and thermal loads. Some of the myriad applications of the pillar substrates in the biological context, especially in cell mechanics (Fig. 7), are reviewed in this section and listed in Table 1.

4.2.1. Microscale applications

The earliest study in the literature employing pillar substrates was presented by Tan et al., where interaction between cells and micropillar substrates was investigated using pillars of 3 μm diameter, 11 μm height, and 6 μm spacing (Tan et al., 2003). Traction forces applied by cells were determined from deflection of the pillars (Fig. 7a) and these traction forces were correlated with the distribution of focal adhesion on each pillar. Traction forces increased with the focal adhesion size for adhesion sites larger than 1 μm^2, whereas there was no such correlation for the adhesion sites smaller than 1 μm^2. Cell response to substrate rigidity (Fig. 7b) (Fu et al., 2010; Ghassemi et al., 2008) and direction dependent rigidity (Fig. 7c) (Saez et al., 2007) were also studied in the literature by changing pillar geometry, where alterations in pillar geometry corresponded to a change in stiffness.

Sniadecki et al. applied an external magnetic field to deflect nanowire embedded micropillars with adhered cells (Sniadecki et al., 2007) (Fig. 7d). The results showed that application of a step force increases the focal adhesion size at the location of the force, but not at the nearby nonmagnetic pillars. Application of such a force caused a loss in contractility at discrete locations of the cell periphery.

Rabodzey et al. investigated the shear forces induced at cell–cell junctions during the neutrophil transmigration of vascular endothelium by growing a confluent endothelial layer on micropillar arrays (2 μm diameter, 3.3 μm to 4.7 height and 4 μm spacing) in an in vitro laminar flow model (Rabodzey et al., 2008) (Fig. 7e). An increase in cell–cell junction forces was observed during intercellular penetration of neutrophils and formation of the gap. In addition, an increase in traction forces

Please cite this article as: Alapan, Y., et al., Micro- and nanodevices integrated with biomolecular probes, Biotechnol Adv (2015), http://dx.doi.org/10.1016/j.biotechadv.2015.09.001

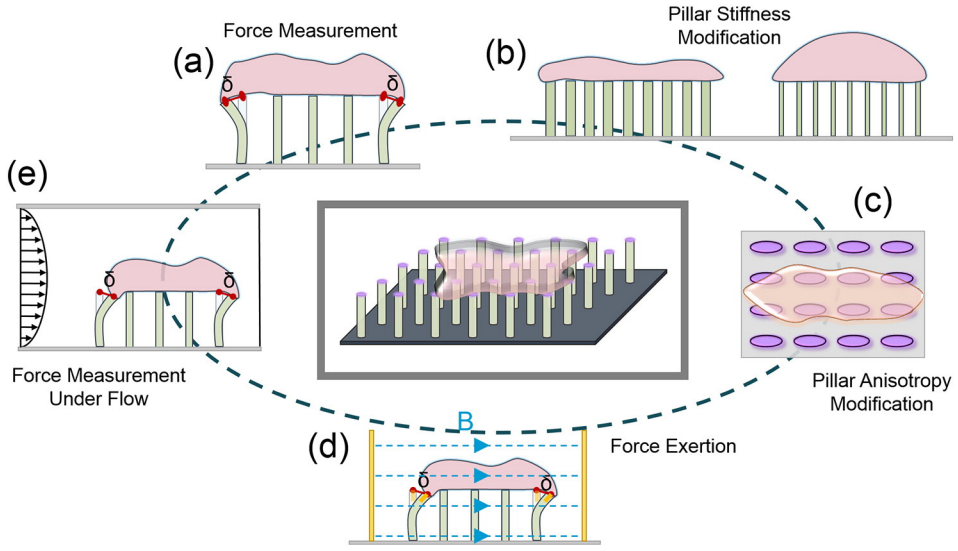

Fig. 7. Micro/nanopillar substrates are versatile tools that can be adapted to the study of various biophysical phenomena. Micro/nanopillar structures are utilized for force measurement by exploiting pillar deflection due to traction of cells adhered on top surfaces of the pillars. (a) Traction force measurement of cells in static conditions, where cells attach and spread on micropillar substrate. (b, c) Pillar substrates can also be modified to study effects of change in biophysical environment of cells. (b) On stiff micropillars, with greater pillar diameter, cells spread on the substrate, whereas displaying a rounded morphology on soft micropillars with smaller pillar diameter. (c) On anisotropically stiff micropillars cells grow in the stiff direction. (d) Nanowire embedded pillar structures can be used to exert forces on cells that are adhered to micropillar top surfaces via an external magnetic field. (e) Traction force measurement of cells under flow conditions can be performed using micropillars to study cell–cell and cell–substrate interactions in vessels.

applied by endothelial cells in response to the penetration and destruction of cell junctions was reported. Furthermore, results showed an increase in traction forces at the transmigration site with increased substrate rigidity. Based on these results, it was suggested that a successful transmigration of a neutrophil through the endothelial monolayer depends on the competition between the cell–cell junctions and cell–substrate interactions.

4.2.2. Nanoscale applications

Kuo et al. utilized nanopillars, ranging from 50 nm to 600 nm in diameter, as a nanocontact printing tool to form fibronectin nanoarrays (Kuo et al., 2011). These nanoarrays were then used to investigate the relation between the size of fibronectin pattern and focal adhesion of Chinese hamster ovary (CHO) cells. It was observed that cells were able to adhere and spread even on the nanoarrays with 50 nm diameter. Furthermore, decrease in average focal adhesion size was reported with the decrease in nanoarray size.

Bucaro et al. investigated the relationship between the geometry of nanopillars (spacing and aspect ratio) and stem cell morphology (Bucaro et al., 2012). Nanopillar arrays with dimensions ranging from 0.2 μm to 0.5 μm in diameter, 5 μm to 10 μm in height, and 0.8 μm to 5 μm in spacing were fabricated. Based on the results, the authors proposed a critical spacing distance, at which extensions of the cells could only grow in the direction where the inter-pillar distances were the shortest. Subcritical spacing led cells to spread radially, because focal adhesions could be established in any direction. On the other hand, with spacing well above the critical spacing distance, cells showed no bridging over the nanopillars. Instead, the cells spread at the base of the nanopillars with increased branching of the extensions. Moreover, the authors reported a dramatic increase in cell polarization with increase in aspect ratio of the pillars, thus reduction in bending stiffness.

5. Microfluidics

Identification and analysis of phenotypic subpopulations of cells and proteins from heterogeneous mediums, such as blood and other bodily fluids, are increasingly growing demands for most of the clinical medicine and basic science research (Jebrail and Wheeler, 2009; Sin et al., 2005). In clinical medicine, such identification could be useful for fast and economic diagnostics, and monitoring of diseases, such as $CD4^+$ cell count for human immunodeficiency virus (HIV) monitoring (Moon et al., 2011) and CTC enumeration for cancer diagnostics (Nagrath et al., 2007). In the last two decades, microfluidic devices integrated with biomolecular probes emerged as a powerful method for highly efficient cell isolation and focused proteomic/genomic analyses (Gurkan et al., 2011a; Kotz et al., 2010; Vickers et al., 2012). Cell isolation in microfluidic devices is generally based on capture of specific cells from a flowing medium (e.g., unprocessed blood) via a biomolecular probe (e.g., antibodies or ECM proteins) functionalized surface. Biological signals, number of isolated cells, and characteristics of cells can be detected using optical and electrical methods (Adams et al., 2008; Gurkan et al., 2011a; Hassan and Bashir, 2014; Moon et al., 2011; Nagrath et al., 2007; Watkins et al., 2013). Microfluidic platforms have overcome the limitations of conventional cell isolation techniques (e.g., fluorescent activated cell sorting, magnetically activated cell sorting) due to their simple and easy use, cost and labor efficient operation, short processing time, high surface to volume ratio, and preprocessing-free use (Murthy et al., 2004). Furthermore, since there are no fluorescent dye or magnetic beads binding to cells, microfluidic systems provide a label-free isolation approach. In this section design/fabrication and biomolecular probe functionalization approaches in microfluidic devices, and various applications in diagnostics, monitoring and regenerative medicine are reviewed.

5.1. Design and fabrication of microfluidic devices

Microfluidic devices with various geometrical designs and dimensions have been utilized in the literature. Dimensions for the channel height are generally reported to be in the range of 50 μm to 500 μm, whereas dimensions for length and width of channels have been reported to be in the micrometer to centimeter range (Alapan et al., 2014; Du et al., 2007; Gurkan et al., 2011a, 2012; Singh et al., 2013; Stott et al., 2010). Geometrical designs utilized for the microfluidic channels can be categorized as: overall chip structure design shaping the flow pathway, and surface structure design to control fluid–structure interaction inside the chip (Fig. 8). Furthermore, to increase the throughput of the microfluidic systems, multiple channels can be used in parallel or in radial arrangements (Gurkan et al., 2011a; Sin et al., 2005; Stott et al., 2010).

Please cite this article as: Alapan, Y., et al., Micro- and nanodevices integrated with biomolecular probes, Biotechnol Adv (2015), http://dx.doi.org/10.1016/j.biotechadv.2015.09.001

Table 1
Microengineered systems integrated with biomolecular probes for measurement of cellular forces and as a controlled environment to study cell–ECM interactions.

Tool	Working principle	Advantages	Disadvantages	Sensitivity	Applications
Micropillars	Forces are measured by imaging the deflections of pillar structures under cells	Precisely controlled substrate properties, simple measurement	Nontrivial topology that might affect cell adhesion for certain geometrical configurations	Reported resolution: 50 pN–12 nN	Smooth muscle, endothelial and fibroblast focal adhesion tractions (Tan et al., 2003), myogenic cell adherens junction forces (Ganz et al., 2006), epithelial focal adhesion tractions during migration (du Roure et al., 2005), cardiac myocyte contractions (Kajzar et al., 2008)
Micropillars in flow chamber	Forces are measured by imaging the deflections of pillar structures under cells, where whole substrate is placed in a flow chamber	Precisely controlled substrate properties, simple measurement	Nontrivial topology that might affect cell adhesion for certain geometrical configurations	Minimum measured force: 1.5 nN–4.5 nN	Effects of laminar or disturbed flow on traction forces of endothelium (Ting et al., 2012), tangential forces at cell–cell junctions during transendothelial neutrophil migration (Rabodzey et al., 2008)
Cantilevers	Forces measured by imaging the deflections of horizontally aligned cantilevers and attached pads under the cells	Simple measurement	Limited to the forces at only one direction and location	Minimum measured force: 3 nN	Fibroblast focal adhesion tractions (Galbraith and Sheetz, 1997)
Bead embedded 2D substrates	Forces are calculated through deformations of beads embedded in substrate exerted by cells	Continuous, native tissue-like substrate	Computationally intensive, coupled mechanical and physical characteristics	Reported resolution: 2 nN–50 pN/μm^2	Fibroblast focal adhesion tractions (Balaban et al., 2001; Dembo and Wang, 1999)
Bead embedded 3D substrates	Forces are calculated through deformations of beads embedded in substrate exerted by cells	Continuous, native tissue-like substrate, three-dimensional environment	Computationally intensive, coupled mechanical and physical characteristics	Sensitivity: 25–75 pN/μm^2	Fibroblast focal adhesion tractions (Legant et al., 2010)
Magnetic micropillars	Cobalt nanowire embedded micropillars act as an actuator under magnetic field	Force application and measurement in the same device, exertion of nanonewton forces	Uncontrollable spatial wire distribution in the substrate	Minimum applied force: 1.3 nN	Response of fibroblast focal adhesion tractions to external force application (Sniadecki et al., 2007)
Anisotropic micropillars	Oval micropillars for anisotropic stiffness in substrate	Direction dependent stiffness modification	Nontrivial topology that might affect cell adhesion for certain geometrical configurations	Minimum stiffness anisotropy: 3	Directional epithelial growth and migration (Saez et al., 2007)
Soft-stiff micropillars	Micropillar substrates with various geometries resulting in various levels of stiffness	Simple modification of substrate rigidity	Nontrivial topology that might affect cell adhesion for certain geometrical configurations	Minimum stiffness: 0.85–1.31 nN/μm	Osteogenic or adipogenic stem cell differentiation (Fu et al., 2010), migration and morphology of fibroblasts and stem cells with respect to substrate rigidity (Ghassemi et al., 2008)

Specific functional designs were utilized in microfluidic studies such as the Hele-Shaw channel, parallel flow channel, and spiral channel designs (Fig. 8). Hele-Shaw channel's lateral shape is designed specifically so that shear stress decreases along the channel length (Fig. 8a), which allows characterization of shear stress dependent parameters, such as cell capture efficiency (Murthy et al., 2004). On the other hand, parallel flow channel design provides a constant flow with increased surface area to capture target cells in parallel serpentine shaped channels (Fig. 8b) and is advantageous in space-constrained settings (Sin et al., 2005). Most of the microfluidic devices employ rectangular prism shaped channels for simplicity in fabrication and operation (Fig. 8c). Similar to the parallel flow channel design, spiral channels (Fig. 8d) also offer constant flow with increased surface area for isolation of specific cells (Vickers et al., 2012).

Even though the earlier microfluidic systems mainly relied on flat surfaces, recent innovative approaches include pillar shaped structures (microposts) or surface ridges (herringbones) (Fig. 8e&f). Antibody functionalized micropillars in microfluidic channels were utilized to increase overall surface area and to enhance target cell–surface interactions, thus improving the capture efficiency of rare CTCs from blood (Hansmann et al., 2011; Nagrath et al., 2007; Ohnaga et al., 2013). Moreover, other studies improved the cell–probe functionalized surface interactions by utilizing microposts from ultra-high porosity CNT forests (Chen et al., 2012). Furthermore, herringbones on channel walls were used to disrupt streamlines of flow and, thus, enhance cell–surface interactions and capture efficiency (Deng et al., 2014; Stott et al., 2010).

5.2. Biomolecular probe functionalization of microfluidic devices

Biomolecular probe functionalization is a critical step for cell adhesion and isolation in microfluidic channel surfaces. Functionalization is a nanoscale process by its nature. For the probe functionalization, either specific antibodies (Alapan et al., 2015; Nagrath et al., 2007; Wang et al., 2012) or ECM proteins (Alapan et al., 2014; Singh et al., 2013) can be immobilized on the microfluidic channel surface. The main difference between antibodies and ECM proteins is that antibodies target specific cell surface antigens, whereas ECM proteins mainly target integrin, a general adhesion receptor on the membrane of cells (Fig. 2). Since antibodies can target specific membrane antigens, antibody functionalization is widely utilized in the literature for highly selective cell isolation and is the main focus of this section.

Functionalization of antibodies on microchannel surface is an integral and critical component of the cell isolation process. In literature, a general approach is to silanize (e.g., (3-Mercaptopropyl)trimethoxysilane or (3-Aminopropyl)triethoxysilane) the channel surface and to add a coupling agent, such as GMBS (N-γ-maleimidobutyryloxy succinimide ester), as the first two steps. Afterwards, linking proteins, such as NeutrAvidin, streptavidin, and Protein G, can be attached to the coupling agent for enhanced capture efficiency or antibodies can be injected directly or with a spacer, such as polyethylene glycol (PEG). Some of the studies utilized PEG to prevent non-specific binding of untargeted cells to the antibodies (Murthy et al., 2004; Vickers et al., 2012). As the last step, the channel surface can be coated with BSA to block non-specific adhesion of untargeted biomolecules and cells.

Biophysical characteristics of antibodies, such as antibody orientation, are also a critical factor in cell isolation efficiency. If an antibody binds to a linking protein by the same domain it binds to a cell antigen, probability of cell interaction and capture decreases. In a recent study (Wang et al., 2012), linking proteins NeutrAvidin and Protein G were compared in terms of antibody orientation and binding efficiency. It was predicted that lower difference in surface roughness before and after the antibody functionalization indicated a more uniform antibody distribution on the surface, which indicates a better capture efficiency. The results showed that Protein G binding protein provides a better antibody orientation than the NeutrAvidin (Fig. 9a–d). This new approach

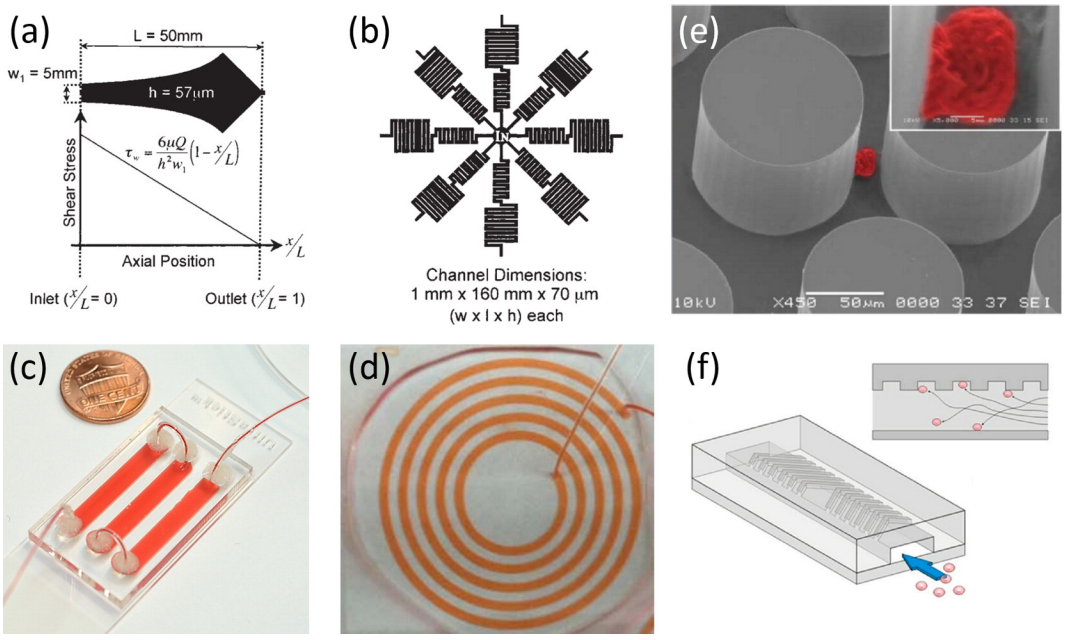

Fig. 8. Structural designs utilized for microfluidic devices. (a–d) Various designs for flow pathway adapted for; measuring shear dependence in (a) Hele-Shaw channels, and increased surface area to facilitate cell–surface interaction in (b) parallel flow channels, (c) rectangular prism channels, and (d) spiral channels. Moreover, internal structures can be utilized to enhance cell–surface interaction using (e) micropost approach, or (f) herringbone mixing design.
Figure sources, used with permission: a and b, Sin et al. (2005); d, Vickers et al. (2012); e, Nagrath et al. (2007); and f, Stott et al. (2010).

was used to isolate individual HIV virus particles from blood with high efficiency and specificity.

5.3. Applications of biomolecular probe functionalized microfluidics

Isolation of specific cell types efficiently and selectively using microfluidic devices from biological fluids, such as blood or synovial fluid, opened up new horizons in clinical medicine. Advancements in microfluidics led to the development of microdevices integrated with biomolecular probes for diagnosis, monitoring, and treatment of diseases, including $CD4^+$ T cell count for point-of-care HIV monitoring (Moon et al., 2011; Wang et al., 2012), separation of CTCs for cancer diagnostics and monitoring (Du et al., 2007; Nagrath et al., 2007; Stott et al., 2010), and purification of stem cells for regenerative medicine (Gurkan et al., 2011a; Plouffe et al., 2009).

For monitoring of HIV patients in anti-retroviral therapy, Moon et al. developed a microscope-free microfluidic chip platform for rapid (under 10 min) separation and enumeration of $CD4^+$ T cells from whole blood (Moon et al., 2011). Microfluidic devices were fabricated in the U.S. with a material cost of less than $1.00 and were shipped

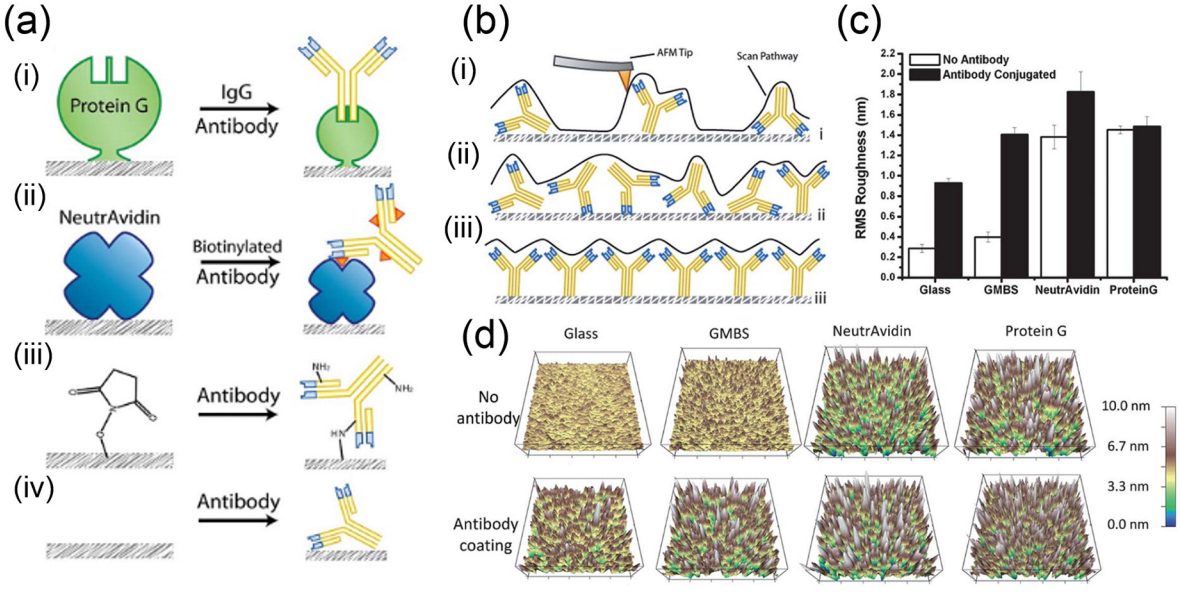

Fig. 9. Effects of binding proteins on antibody orientation. (a) Different immobilization methods: Antibody binding to (i) Protein G and (ii) NeutrAvidin, (iii) GMBS, and (iv) directly to plain glass surface. (b) Illustration of the AFM analyses: (i) low antibody density, (ii) high density randomly oriented antibodies, and (iii) high density uniformly oriented antibodies. (c) Surface roughness of different immobilization methods determined by AFM. (d) Surface morphology is modified with different functionalization approaches.
Figure source, used with permission: Wang et al. (2012).

to Tanzania for field testing by minimally trained personnel in a resource-limited setting. The results showed a correlation between measurements of the microfluidic device with the flow cytometry system, both in the U.S. and in Tanzania.

Nagrath et al. developed a micropost based microfluidic device to isolate CTCs, which were in the range of 1–100 in 1 mL of blood compared to 3–6 $\times 10^9$ RBCs (Dharmasiri et al., 2010), as a potential method for the detection and monitoring of non-hematologic cancers (Nagrath et al., 2007). The microfluidic device isolated CTCs from unprocessed blood samples of patients with various cancer types (lung, prostate, pancreatic, breast and colon cancers) on antibody (EpCAM) functionalized microposts with 50% purity. The microfluidic device identified CTCs in 115 of 116 samples from patients with various cancer types. Furthermore, in a small group of patients taking systematic treatment, the number of captured CTCs was well correlated with the clinical course of the disease.

Gurkan et al. developed a microfluidic device with the capability of not only isolating specific cell types but also retrieving the captured cells from the microfluidic channels on-demand (Gurkan et al., 2011a). Cell retrieval was enabled through coating of the glass surface with a temperature responsive polymer (poly(N-isopropylacrylamide), PNIPAAm) that can absorb antibodies at 37 °C and desorb them at temperatures lower than 32 °C. After the target cells were captured on surface functionalized antibodies at 37 °C, cell binding antibodies were desorbed along with cells by cooling the temperature below 32 °C. $CD34^+$ endothelial progenitor cells, which are extremely low in number in the blood, were isolated and retrieved in the microfluidic channels on antibody (anti-CD34) functionalized surfaces with 90% specificity and more than 90% viability.

High throughput along with high selectivity (specificity) is considered to be the ultimate goal of microfluidic cell isolation systems. Even though cell isolation from whole blood can be achieved in microfluidic devices, depletion of non-target cell types beforehand can increase selectivity and throughput. However, sample preparation steps for non-target cell depletion require additional reagents, infrastructure, and labor. To eliminate these extra sample preparation steps, several studies either integrated physical separation modalities (Karabacak et al., 2014; Ozkumur et al., 2013) or miniaturized chemical means of removal of non-target cells (Watkins et al., 2013) as an integral part of the microfluidic platform.

6. Current challenges and other micro/nanodevices

In the previous sections we reviewed cantilevers, micro/nanopillars, and microfluidic systems in detail. There are other promising micro/nanotools that are enabled by biomolecular probes. Nanowires are another example of label-free, microfabricated biosensors. They are mostly designed as nanowire field effect transistors (nanowire FETs). Nanowire FET structure is similar to conventional FET, which includes a drain, a source, a semiconductor channel, and gate electrodes. Nanowire forms the semiconductor channel with a high surface area-to-volume ratio. The binding of biomolecules to the nanowire causes the accumulation or depletion of charge carriers both on the wire surface and inside the wire resulting in detectable conductivity changes. Silicon, indium oxide and carbon nano tubes (CNTs) are commonly used in nanowire FETs (Li et al., 2005; Tang et al., 2005). CNTs can be fabricated as single walled (every carbon atom located on the surface of the nanotubes) or multi-walled. Single walled CNTs (SWCNT) demonstrate ultra-high sensitivity because of their size (~1 nm diameter). By using silicon or indium oxide FETs, antibodies (Stern et al., 2007), ssDNA (Kim et al., 2007), virus (Patolsky et al., 2004), proteins (Cui et al., 2001), and electrical activities of neuron cells (Patolsky et al., 2006) have been detected while by using CNT FETs protein (Maehashi et al., 2007), antibody (Li et al., 2005), glucose (Besteman et al., 2003), and DNA (Li et al., 2003) have been detected.

Although nanowire biosensors have ultrahigh sensitivity and portability, device performance highly depends on the ionic concentration and ionic strength of the buffer solution. Ionic strength of the buffer solution determines an important parameter, the Debye length for FET based nanowires (Maehashi et al., 2007). In order to sense the charge of the target molecules with higher sensitivity, binding should occur close to the sensor surface; shorter than the Debye length. Usually low ionic strength buffer solutions are used to increase the Debye length. However, some biomolecular reactions require high ionic strength such as DNA hybridization buffers and untreated serum. This problem is an inherent limitation for nanowire sensors; in addition to their extreme susceptibility to nonspecific entities that are present in complex mixtures.

Surface plasmon resonance (SPR) operation relies on monitoring the surface plasmon waves (SPWs) to detect receptor–target molecule interactions at the surface of a metallic film or nanoparticles. In a typical SPR system, receptor molecules are immobilized on a metal film. The receptor-modified metal film (usually gold) interacts with the flow within the channel, where the other side is in contact with a glass slide that allows the incident light through. At certain wavelengths and angles, incident light passes through glass slide and excites SPW at the interface of metal film and biomolecules. At a certain incident angle (resonant angle), SPW adsorbs the energy which results in a minimum intensity of the reflected light. SPW is very sensitive to changes in the refractive index of the sensor surface caused by biomolecular interactions. Thus, molecular binding events at the sensor surface can be detected by measuring the changes in resonant angle. SPR operates in real-time and detects target molecules in aqueous solutions (Hoa et al., 2007; Karlsson, 2004). The sensitivity of typical SPR systems can be improved by incorporating nanomaterials (Choi and Lee, 2013; Zeng et al., 2014) and alternative approaches, such as local surface plasmon resonance (Cho et al., 2012) and surface-enhanced Raman scattering (Fu et al., 2014; Lu et al., 2005).

For detection and measurement of cell traction forces, various methods have been developed in addition to pillar arrays, such as ultrathin silicone films (Harris et al., 1980; Helfman et al., 1999), and polyacrylamide (PAA) gels (Balaban et al., 2001; Dembo and Wang, 1999). Traction forces are measured on ultrathin films by the distortions and wrinkles that the cells form. Even though this method provided an important insight, force measurement from distorted films is complicated in its nature (Yang et al., 2011). On the other hand, fluorescent microbead embedded PAA gels provide a more accurate quantification of the traction forces (Table 1). Dembo and Wang studied the traction forces at focal adhesions during locomotion of single 3T3 fibroblast cells using collagen conjugated PAA gels with embedded fluorescent marker beads (Dembo and Wang, 1999). Moreover, stiffness of the gel can be tuned via changing the level of cross-linking. However changing the level of cross-linking not only alters the mechanical properties of the substrate but also has an effect on the porosity, surface chemistry and binding properties of the ligands (Fu et al., 2010). This coupling between different material properties somewhat limits the use of gels for cell–substrate interaction studies.

Even though micropillar substrates provide sensitivity and versatility, they are limited in mimicking the natural cell microenvironment due to their 2D configuration, whereas cells are in 3D matrices in-vivo. This dimensional problem is a limiting factor for gel substrates as well. To overcome this issue, Legant et al. adapted the bead embedded gel approach into a 3D elastic hydrogel matrix to study traction forces of EGFP-expressing 3T3 fibroblasts (Legant et al., 2010). Even though a 3D environment was produced for the cells, this approach is susceptible to computationally intensive data processing. In another study, prebent, flexible, and ECM protein functionalized cantilevers in a blossoming flower configuration were fabricated to measure traction forces of cells in 3D (Marelli et al., 2014). A limitation of this method is the restriction of cells in a confined configuration, which does not allow cell migration and cell–cell interactions.

Please cite this article as: Alapan, Y., et al., Micro- and nanodevices integrated with biomolecular probes, Biotechnol Adv (2015), http://dx.doi.org/10.1016/j.biotechadv.2015.09.001

Microfluidic systems that rely on physical characteristics of cells have also been utilized for cell isolation without surface functionalization. These techniques include physical filtration, inertial focusing, dielectrophoresis, acoustophoresis, and optical tweezers. Cell isolation methods based on physical filtration take advantage of the differences in size and deformability of different cell types. Physical filtration has been utilized in isolation of cell populations, such as monocytes (Chen et al., 2013), and CTCs (Lin et al., 2010; Xu et al., 2010). Inertial focusing exploits inertial forces resulting from fluid flow in a channel. Shear-gradient lift and wall-induced lift result in a net force that brings the cells to an equilibrium position (Di Carlo, 2009; Yu et al., 2014). Through this motion, a homogenously dispersed cell stream can be aligned in a focused stream, which was then utilized for isolation of platelets (Di Carlo et al., 2008), and CTCs (Bhagat et al., 2011; Hou et al., 2013) in microfluidic channels. Dielectrophoresis is the movement of dielectric particles in a non-uniform electric field. The electric field polarizes the particles and their movement occurs due to the interaction between the particle's dipoles and the spatial gradient of the electric field (Cetin and Li, 2011). This phenomenon has been utilized in microfluidic channels for isolation of cell populations, such as platelets (Pommer et al., 2008) and CTCs (Alazzam et al., 2011; Gupta et al., 2012). Acoustophoresis is based on manipulation of cells using ultrasound radiation forces generated in an acoustically soft medium within an acoustically rigid microchannel. These ultrasound radiation forces drive cells toward the pressure nodes or anti-pressure nodes of the acoustic field (Augustsson et al., 2012; Lin et al., 2012; Yu et al., 2014). Acoustophoresis has been utilized for isolation of platelets (Nam et al., 2011) and CTCs (Li et al., 2015). Aside from these approaches, optical tweezers have also been utilized in microfluidic channels for separation of cells. Optical tweezers are based on tightly coupled laser light to manipulate dielectric microparticles (Wang et al., 2011). Feasibility of cell isolation in microfluidic channels using optical tweezers has been shown by separation of fluorescently labeled HeLa cells (Wang et al., 2005), macrophages (Perroud et al., 2008), and human embryonic stem cells (Wang et al., 2011).

The techniques summarized above provide high-throughput processing of blood while relying on physical properties of cells for separation, such as size, density, electrical polarizability, and compressibility. Even though these physical properties can be considered as a biomarker to some extent, specificity and selectivity still remain as challenges in these techniques. Whereas, antigen–antibody interactions can be deemed as the specific fingerprints of cells and these interactions are also the key components of the natural selectivity mechanism in the body. In recent years, studies taking advantage of both physical properties and antigen–antibody interactions of cells have been performed for high throughput isolation along with high selectivity (Chang et al., 2015; Karabacak et al., 2014; Ozkumur et al., 2013).

Biofouling in micro- and nanodevices is generally regarded as nonspecific binding of molecules or cells to the device surface, which can affect the sensitivity and selectivity of the device (Yoon and Garrell, 2014). Advances in both sensor designs and functionalization methods resulted in obtaining higher yields for specific binding. For example, differential cantilever design together with inkjet printing methods for functionalization of the surface offers improved experimental performance (Icoz et al., 2008). On the other hand, most of the microfluidic platforms integrated with biomolecular probes utilized blocking agents, such as bovine serum albumin (BSA) to prevent non-specific binding events (Alapan et al., 2014; Bai et al., 2006; Cheng et al., 2007; Gurkan et al., 2011a, 2012; Wang et al., 2012). It is evident that research on surface chemistry and molecular interactions are becoming more significant as fabrication methods for new generation biosensors are standardized.

7. Summary and future perspectives

Micro/nanotools integrated with biomolecular probes interact with nucleic acids, proteins, and cells, and convert the interaction between the biological target and the biomolecular probe into a measurable signal. These new tools and capabilities allow the analysis and measurement of the target at biologically relevant scales. Every transducer type (e.g., cantilever, nanowire, pillar) relies on a different physical phenomenon, such as changes in mechanical (e.g., deflection, strain, surface tension), electrical (e.g., conductivity, current, capacitance), or optical (e.g., intensity, reflection) properties. As micro- and nanotechnologies open new horizons for advanced fabrication methods, researchers are able to design and produce novel transducers with improved sensitivity, throughput, and specificity. Through these improvements, translation of the micro/nanotools from laboratories to the field is becoming more feasible. In order to commercialize new generation biosensors, additional optimization efforts are needed in two fronts: (i) enhanced selectivity of sensing tools while handling complex media, such as blood, and (ii) improved functionalization of the device surface with precisely controlled dense arrays of appropriate biomolecular probes. Experimental studies need to be supported with analytical tools and theoretical methods to improve the response of the micro/nanotools (Nair and Alam, 2010). Computer aided simulations may be used to guide the advancement of the device design and to determine the operational limits of the system. Experimental procedures are usually optimized by iterative steps, which consume time, effort and materials. Theoretical studies may reduce the needed resources to develop and optimize biosensors (Kim and Zheng, 2008).

The overall aim of developing new generation transducers is to achieve portable, low cost, and highly sensitive devices to replace current cost and time consuming technologies. For example, effective utilization of microfluidic technologies as cost and time efficient biosensing platforms in underdeveloped countries could be a milestone for point-of-care diagnosis and monitoring of millions of patients with restricted access to health care facilities. Even in the developed world, microfluidic platforms have the potential to revolutionize clinical medicine by improving the diagnostics and monitoring of diseases, such as cancer, and HIV, into simple and fast procedures, which could enable early diagnosis and improve the quality of patients' life. Despite all the developments in micro/nanotools biosensors, these new systems are still facing limitations in sensitivity, efficiency, and parallel processing of biological samples. In general, analysis of only one property is not sufficient in biological analyses or in clinical medicine to determine a clear outcome. Therefore, releasing/recovering the analyzed sample out of the device for further analyses, or running multiple analyses in the same device is still among the major challenges. The micro/nanotools and technologies presented here demonstrate potential in biology and medicine, especially in sensing of biological components, ranging from proteins to cells. Such methods integrate advanced micro/nanofabrication methods to achieve enhanced sensitivity and control. Throughput, speed, scalability, user friendliness, cost of fabrication and utilization of these tools and methods still have plenty of room for improvement. Development of micro/nanotools has rightfully been the research focus of many laboratories for many years now. It is certain that we will continue to be amazed with the advancements and the pioneering and lifesaving possibilities offered by these tools.

Acknowledgments

This work was supported in part by Grant # 2013126 from the Doris Duke Charitable Foundation, Coulter-Case Translational Research Partnership Award, Steven Garverick Memorial Innovation Incentive Award, and an award from the Clinical and Translational Science Collaborative (CTSC) of Cleveland: UL1TR000439 from the National Center for Advancing Translational Sciences (NCATS) component of the National Institutes of Health (NIH) and NIH roadmap for Medical Research. Its contents are solely the responsibility of the authors and do not necessarily represent the official views of the NIH. Y. A. and U. A. G. acknowledge the Center for Integration of Medicine & Innovative Technology (CIMIT) Student Technology Prize for Primary Healthcare. U. A. G.

would like to thank the University Center for Innovation in Teaching and Education (UCITE) for the Glennan Fellowship, which supports the Scientific Art Program and art student internship at Case Biomanufacturing and Microfabrication Laboratory. The authors acknowledge Bin-Da Chan and Cagri Savran from Purdue University for their help in the preparation of Fig. 3a, and Selim Ozden for his help in preparing Fig. 3b and Fig. 5c.

References

Adams, A.A., Okagbare, P.I., Feng, J., Hupert, M.L., Patterson, D., Gottert, J., et al., 2008. Highly efficient circulating tumor cell isolation from whole blood and label-free enumeration using polymer-based microfluidics with an integrated conductivity sensor. J. Am. Chem. Soc. 130, 8633–8641.

Adkins, J.N., Varnum, S.M., Auberry, K.J., Moore, R.J., Angell, N.H., Smith, R.D., et al., 2002. Toward a human blood serum proteome: analysis by multidimensional separation coupled with mass spectrometry. Mol. Cell. Proteomics 1, 947–955.

Alapan, Y., Little, J.A., Gurkan, U.A., 2014. Heterogeneous red blood cell adhesion and deformability in sickle cell disease. Sci. Rep. 4, 7173.

Alapan, Y., Hasan, M.N., Shen, R., Gurkan, U.A., 2015. Three-dimensional printing based hybrid manufacturing of microfluidic devices. J. Nanotechnol. Eng. Med. http://dx.doi.org/10.1115/1.4031231.

Alazzam, A., Stiharu, I., Bhat, R., Meguerditchian, A.N., 2011. Interdigitated comb-like electrodes for continuous separation of malignant cells from blood using dielectrophoresis. Electrophoresis 32, 1327–1336.

Alvarez, M., Tamayo, J., 2005. Optical sequential readout of microcantilever arrays for biological detection. Sensors Actuators B Chem. 106, 687–690.

Angst, B.D., Marcozzi, C., Magee, A.I., 2001. The cadherin superfamily: diversity in form and function. J. Cell Sci. 114, 629–641.

Aplin, A.E., Howe, A., Alahari, S.K., Juliano, R.L., 1998. Signal transduction and signal modulation by cell adhesion receptors: the role of integrins, cadherins, immunoglobulin–cell adhesion molecules, and selectins. Pharmacol. Rev. 50, 197–263.

Arntz, Y., Seelig, J.D., Lang, H.P., Zhang, J., Hunziker, P., Ramseyer, J.P., et al., 2003. Label-free protein assay based on a nanomechanical cantilever array. Nanotechnology 14, 86–90.

Atalay, Y.T., Vermeir, S., Witters, D., Vergauwe, N., Verbruggen, B., Verboven, P., et al., 2011. Microfluidic analytical systems for food analysis. Trends Food Sci. Technol. 22, 386–404.

Augustsson, P., Magnusson, C., Nordin, M., Lilja, H., Laurell, T., 2012. Microfluidic, label-free enrichment of prostate cancer cells in blood based on acoustophoresis. Anal. Chem. 84, 7954–7962.

Bai, Y., Koh, C.G., Boreman, M., Juang, Y.J., Tang, I.C., Lee, L.J., et al., 2006. Surface modification for enhancing antibody binding on polymer-based microfluidic device for enzyme-linked immunosorbent assay. Langmuir 22, 9458–9467.

Balaban, N.Q., Schwarz, U.S., Riveline, D., Goichberg, P., Tzur, G., Sabanay, I., et al., 2001. Force and focal adhesion assembly: a close relationship studied using elastic micropatterned substrates. Nat. Cell Biol. 3, 466–472.

Barabino, G.A., McIntire, L.V., Eskin, S.G., Sears, D.A., Udden, M., 1987a. Endothelial cell interactions with sickle cell, sickle trait, mechanically injured, and normal erythrocytes under controlled flow. Blood 70, 152–157.

Barabino, G.A., McIntire, L.V., Eskin, S.G., Sears, D.A., Udden, M., 1987b. Rheological studies of erythrocyte–endothelial cell interactions in sickle cell disease. Prog. Clin. Biol. Res. 240, 113–127.

Battiston, F.M., Ramseyer, J.P., Lang, H.P., Baller, M.K., Gerber, C., Gimzewski, J.K., et al., 2001. A chemical sensor based on a microfabricated cantilever array with simultaneous resonance-frequency and bending readout. Sensors Actuators B Chem. 77, 122–131.

Besteman, K., Lee, J.O., Wiertz, F.G.M., Heering, H.A., Dekker, C., 2003. Enzyme-coated carbon nanotubes as single-molecule biosensors. Nano Lett. 3, 727–730.

Bhagat, A.A., Hou, H.W., Li, L.D., Lim, C.T., Han, J., 2011. Pinched flow coupled shear-modulated inertial microfluidics for high-throughput rare blood cell separation. Lab Chip 11, 1870–1878.

Bietsch, A., Zhang, J.Y., Hegner, M., Lang, H.P., Gerber, C., 2004. Rapid functionalization of cantilever array sensors by inkjet printing. Nanotechnology 15, 873–880.

Bronzino, J.D., 2000. The Biomedical Engineering Handbook. 2nd ed. CRC Press, Boca Raton, FL.

Bucaro, M.A., Vasquez, Y., Hatton, B.D., Aizenberg, J., 2012. Fine-tuning the degree of stem cell polarization and alignment on ordered arrays of high-aspect-ratio nanopillars. ACS Nano 6, 6222–6230.

Burg, T.P., Godin, M., Knudsen, S.M., Shen, W., Carlson, G., Foster, J.S., et al., 2007. Weighing of biomolecules, single cells and single nanoparticles in fluid. Nature 446, 1066–1069.

Calleja, M., Tamayo, J., Nordstrom, M., Boisen, A., 2006. Low-noise polymeric nanomechanical biosensors. Appl. Phys. Lett. 88.

Cavallaro, U., Christofori, G., 2004. Cell adhesion and signalling by cadherins and Ig-CAMs in cancer. Nat. Rev. Cancer 4, 118–132.

Cetin, B., Li, D., 2011. Dielectrophoresis in microfluidics technology. Electrophoresis 32, 2410–2427.

Chan, B.D., Icoz, K., Gieseck, R.L., Savran, C.A., 2013. Selective weighing of individual microparticles using a hybrid micromanipulator–nanomechanical resonator system. IEEE Sensors J. 13, 2857–2862.

Chan, B.D., Icoz, K., Huang, W., Chang, C.L., Savran, C.A., 2014. On-demand weighing of single dry biological particles over a 5-order-of-magnitude dynamic range. Lab Chip 14, 4188–4196.

Chang, J., Shi, P.A., Chiang, E.Y., Frenette, P.S., 2008. Intravenous immunoglobulins reverse acute vaso-occlusive crises in sickle cell mice through rapid inhibition of neutrophil adhesion. Blood 111, 915–923.

Chang, C.L., Huang, W., Jalal, S.I., Chan, B.D., Mahmood, A., Shahda, S., et al., 2015. Circulating tumor cell detection using a parallel flow micro-aperture chip system. Lab Chip 15, 1677–1688.

Chen, G.D., Fachin, F., Colombini, E., Wardle, B.L., Toner, M., 2012. Nanoporous micro-element arrays for particle interception in microfluidic cell separation. Lab Chip 12, 3159–3167.

Chen, W., Huang, N.T., Oh, B., Lam, R.H., Fan, R., Cornell, T.T., et al., 2013. Surface-micromachined microfiltration membranes for efficient isolation and functional immunophenotyping of subpopulations of immune cells. Adv. Healthc. Mater. 2, 965–975.

Cheng, X., Irimia, D., Dixon, M., Sekine, K., Demirci, U., Zamir, L., et al., 2007. A microfluidic device for practical label-free CD4(+) T cell counting of HIV-infected subjects. Lab Chip 7, 170–178.

Cho, E.J., Lee, J.-W., Ellington, A.D., 2009. Applications of aptamers as sensors. Annu. Rev. Anal. Chem. 2, 241–264.

Cho, H., Yeh, E.C., Sinha, R., Laurence, T.A., Bearinger, J.P., Lee, L.P., 2012. Single-step nanoplasmonic VEGF165 aptasensor for early cancer diagnosis. ACS Nano 6, 7607–7614.

Choi, I., Lee, L.P., 2013. Rapid detection of Abeta aggregation and inhibition by dual functions of gold nanoplasmic particles: catalytic activator and optical reporter. ACS Nano 7, 6268–6277.

Collings, A.F., Caruso, F., 1997. Biosensors: recent advances. Rep. Prog. Phys. 60, 1397–1445.

Cozens-Roberts, C., Quinn, J.A., Lauffenberger, D.A., 1990. Receptor-mediated adhesion phenomena. Model studies with the radical-flow detachment assay. Biophys. J. 58, 107–125.

Crevillen, A.G., Avila, M., Pumera, M., Gonzalez, M.C., Escarpa, A., 2007. Food analysis on microfluidic devices using ultrasensitive carbon nanotubes detectors. Anal. Chem. 79, 7408–7415.

Cui, Y., Wei, Q.Q., Park, H.K., Lieber, C.M., 2001. Nanowire nanosensors for highly sensitive and selective detection of biological and chemical species. Science 293, 1289–1292.

Dembo, M., Wang, Y.L., 1999. Stresses at the cell-to-substrate interface during locomotion of fibroblasts. Biophys. J. 76, 2307–2316.

den Elzen, N., Buttery, C.V., Maddugoda, M.P., Ren, G., Yap, A.S., 2009. Cadherin adhesion receptors orient the mitotic spindle during symmetric cell division in mammalian epithelia. Mol. Biol. Cell 20, 3740–3750.

Deng, Y., Zhang, Y., Sun, S., Wang, Z., Wang, M., Yu, B., et al., 2014. An integrated microfluidic chip system for single-cell secretion profiling of rare circulating tumor cells. Sci. Rep. 4, 7499.

Dharmasiri, U., Witek, M.A., Adams, A.A., Soper, S.A., 2010. Microsystems for the capture of low-abundance cells. Annu. Rev. Anal. Chem. (Palo Alto, Calif.) 3, 409–431.

Dhayal, B., Henne, W.A., Doorneweerd, D.D., Reifenberger, R.G., Low, P.S., 2006. Detection of *Bacillus subtilis* spores using peptide-functionalized cantilever arrays. J. Am. Chem. Soc. 128, 3716–3721.

Di Carlo, D., 2009. Inertial microfluidics. Lab Chip 9, 3038–3046.

Di Carlo, D., Edd, J.F., Irimia, D., Tompkins, R.G., Toner, M., 2008. Equilibrium separation and filtration of particles using differential inertial focusing. Anal. Chem. 80, 2204–2211.

du Roure, O., Saez, A., Buguin, A., Austin, R.H., Chavrier, P., Silberzan, P., et al., 2005. Force mapping in epithelial cell migration. Proc. Natl. Acad. Sci. U. S. A. 102, 2390–2395.

Du, Z., Cheng, K.H., Vaughn, M.W., Collie, N.L., Gollahon, L.S., 2007. Recognition and capture of breast cancer cells using an antibody-based platform in a microelectromechanical systems device. Biomed. Microdevices 9, 35–42.

El-Sayed, I.H., Huang, X.H., El-Sayed, M.A., 2005. Surface plasmon resonance scattering and absorption of anti-EGFR antibody conjugated gold nanoparticles in cancer diagnostics: applications in oral cancer. Nano Lett. 5, 829–834.

Folch, A., 2012. Introduction to BioMEMS. 1st ed. CRC Press, Boca Raton, FL.

Fritz, J., Baller, M.K., Lang, H.P., Rothuizen, H., Vettiger, P., Meyer, E., et al., 2000. Translating biomolecular recognition into nanomechanics. Science 288, 316–318.

Fu, J., Wang, Y.K., Yang, M.T., Desai, R.A., Yu, X., Liu, Z., et al., 2010. Mechanical regulation of cell function with geometrically modulated elastomeric substrates. Nat. Methods 7, 733–736.

Fu, C., Gu, Y., Wu, Z., Wang, Y., Xu, S., Xu, W., 2014. Surface-enhanced Raman scattering (SERS) biosensing based on nanoporous dielectric waveguide resonance. Sensors Actuators B Chem. 201, 173–176.

Galbraith, C.G., Sheetz, M.P., 1997. A micromachined device provides a new bend on fibroblast traction forces. Proc. Natl. Acad. Sci. U. S. A. 94, 9114–9118.

Ganz, A., Lambert, M., Saez, A., Silberzan, P., Buguin, A., Mege, R.M., et al., 2006. Traction forces exerted through N-cadherin contacts. Biol. Cell. 98, 721–730.

Gao, Z.Q., Agarwal, A., Trigg, A.D., Singh, N., Fang, C., Tung, C.H., et al., 2007. Silicon nanowire arrays for label-free detection of DNA. Anal. Chem. 79, 3291–3297.

Gardel, M.L., Schneider, I.C., Aratyn-Schaus, Y., Waterman, C.M., 2010. Mechanical integration of actin and adhesion dynamics in cell migration. Annu. Rev. Cell Dev. Biol. 26, 315–333.

Ghassemi, S., Biais, N., Maniura, K., Wind, S.J., Sheetz, M.P., Hone, J., 2008. Fabrication of elastomer pillar arrays with modulated stiffness for cellular force measurements. J. Vac. Sci. Technol. B Microelectron. Nanometer Struct. Process. Meas. Phenom. 26, 2549–2553.

Ghassemi, S., Rossier, O., Sheetz, M.P., Wind, S.J., Hone, J., 2009. Gold-tipped elastomeric pillars for cellular mechanotransduction. J. Vac. Sci. Technol. B Microelectron. Nanometer Struct. Process. Meas. Phenom. 27, 3088–3091.

Please cite this article as: Alapan, Y., et al., Micro- and nanodevices integrated with biomolecular probes, Biotechnol Adv (2015), http://dx.doi.org/10.1016/j.biotechadv.2015.09.001

Ghibaudo, M., Saez, A., Trichet, L., Xayaphoummine, A., Browaeys, J., Silberzan, P., et al., 2008. Traction forces and rigidity sensing regulate cell functions. Soft Matter 4, 1836–1843.
Gooding, J.J., 2002. Electrochemical DNA hyhridization biosensors. Electroanalysis 14, 1149–1156.
Grayson, A.C.R., Shawgo, R.S., Johnson, A.M., Flynn, N.T., Li, Y.W., Cima, M.J., et al., 2004. A BioMEMS review: MEMS technology for physiologically integrated devices. Proc. IEEE 92, 6–21.
Griffin, M.F., Butler, P.E., Seifalian, A.M., Kalaskar, D.M., 2015. Control of stem cell fate by engineering their micro and nanoenvironment. World J. Stem Cells 7, 37–50.
Gupta, A., Akin, D., Bashir, R., 2004a. Detection of bacterial cells and antibodies using surface micromachined thin silicon cantilever resonators. J. Vac. Sci. Technol. B 22, 2785–2791.
Gupta, A., Akin, D., Bashir, R., 2004b. Single virus particle mass detection using microresonators with nanoscale thickness. Appl. Phys. Lett. 84, 1976–1978.
Gupta, V., Jafferji, I., Garza, M., Melnikova, V.O., Hasegawa, D.K., Pethig, R., et al., 2012. ApoStream(™), a new dielectrophoretic device for antibody independent isolation and recovery of viable cancer cells from blood. Biomicrofluidics 6, 24133.
Gurkan, U.A., Anand, T., Tas, H., Elkan, D., Akay, A., Keles, H.O., et al., 2011a. Controlled viable release of selectively captured label-free cells in microchannels. Lab Chip 11, 3979–3989.
Gurkan, U.A., Moon, S., Geckil, H., Xu, F., Wang, S., Lu, T.J., Demirci, U., 2011b. Miniaturized lensless imaging systems for cell and microorganism visualization in point-of-care testing. Biotechnol. J. 6, 138–149. http://dx.doi.org/10.1002/biot.201000427.
Gurkan, U.A., Tasoglu, S., Akkaynak, D., Avci, O., Unluisler, S., Canikyan, S., et al., 2012. Smart interface materials integrated with microfluidics for on-demand local capture and release of cells. Adv. Healthc. Mater. 1, 661–668.
Hansmann, G., Plouffe, B.D., Hatch, A., von Gise, A., Sallmon, H., Zamanian, R.T., et al., 2011. Design and validation of an endothelial progenitor cell capture chip and its application in patients with pulmonary arterial hypertension. J. Mol. Med. (Berl.) 89, 971–983.
Harris, A.K., Wild, P., Stopak, D., 1980. Silicone rubber substrata: a new wrinkle in the study of cell locomotion. Science 208, 177–179.
Hassan, U., Bashir, R., 2014. Electrical cell counting process characterization in a microfluidic impedance cytometer. Biomed. Microdevices 16, 697–704.
Hassell, K.L., 2010. Population estimates of sickle cell disease in the U.S. Am. J. Prev. Med. 38, S512–S521.
Hatch, A., Hansmann, G., Murthy, S.K., 2011. Engineered alginate hydrogels for effective microfluidic capture and release of endothelial progenitor cells from whole blood. Langmuir 27, 4257–4264.
Hebbel, R.P., Boogaerts, M.A., Eaton, J.W., Steinberg, M.H., 1980. Erythrocyte adherence to endothelium in sickle-cell anemia. A possible determinant of disease severity. N. Engl. J. Med. 302, 992–995.
Hebbel, R.P., Eaton, J.W., Steinberg, M.H., White, J.G., 1981. Erythrocyte/endothelial interactions and the vasocclusive severity of sickle cell disease. Prog. Clin. Biol. Res. 55, 145–162.
Helfman, D.M., Levy, E.T., Berthier, C., Shtutman, M., Riveline, D., Grosheva, I., et al., 1999. Caldesmon inhibits nonmuscle cell contractility and interferes with the formation of focal adhesions. Mol. Biol. Cell 10, 3097–3112.
Hoa, X.D., Kirk, A.G., Tabrizian, M., 2007. Towards integrated and sensitive surface plasmon resonance biosensors: a review of recent progress. Biosens. Bioelectron. 23, 151–160.
Hong, P., Li, W., Li, J., 2012. Applications of aptasensors in clinical diagnostics. Sensors (Basel) 12, 1181–1193.
Hou, H.W., Warkiani, M.E., Khoo, B.L., Li, Z.R., Soo, R.A., Tan, D.S., et al., 2013. Isolation and retrieval of circulating tumor cells using centrifugal forces. Sci. Rep. 3, 1259.
Howorka, S., Cheley, S., Bayley, H., 2001. Sequence-specific detection of individual DNA strands using engineered nanopores. Nat. Biotechnol. 19, 636–639.
Hu, W., Crouch, A.S., Miller, D., Aryal, M., Luebke, K.J., 2010. Inhibited cell spreading on polystyrene nanopillars fabricated by nanoimprinting and in situ elongation. Nanotechnology 21, 385301.
Huttenlocher, A., Horwitz, A.R., 2011. Integrins in cell migration. Cold Spring Harb. Perspect. Biol. 3, a005074.
Hynes, R.O., 1999. Cell adhesion: old and new questions. Trends Cell Biol. 9, M33–M37.
Icoz, K., Savran, C., 2010. Nanomechanical biosensing with immunomagnetic separation. Appl. Phys. Lett. 97.
Icoz, K., Iverson, B.D., Savran, C., 2008. Noise analysis and sensitivity enhancement in immunomagnetic nanomechanical biosensors. Appl. Phys. Lett. 93.
Ilic, B., Czaplewski, D., Craighead, H.G., Neuzil, P., Campagnolo, C., Batt, C., 2000. Mechanical resonant immunospecific biological detector. Appl. Phys. Lett. 77, 450–452.
Inci, F., Tokel, O., Wang, S., Gurkan, U.A., Kuritzkes, D.R., Demirci, U., 2013a. Nanoplasmonic biosensing platform for multiple pathogen detection. Solid-State Sensors, Actuators and Microsystems (TRANSDUCERS & EUROSENSORS XXVII), 2013 Transducers & Eurosensors XXVII: The 17th International Conference on, pp. 2431–2434.
Inci, F., Tokel, O., Wang, S.Q., Gurkan, U.A., Tasoglu, S., Kuritzkes, D.R., et al., 2013b. Nanoplasmonic quantitative detection of intact viruses from unprocessed whole blood. ACS Nano 7, 4733–4745.
Jebrail, M.J., Wheeler, A.R., 2009. Digital microfluidic method for protein extraction by precipitation. Anal. Chem. 81, 330–335.
Jin, H., Aiyer, A., Su, J., Borgstrom, P., Stupack, D., Friedlander, M., et al., 2006. A homing mechanism for bone marrow-derived progenitor cell recruitment to the neovasculature. J. Clin. Investig. 116, 652–662.
Johnson, L., Gupta, A.T.K., Ghafoor, A., Akin, D., Bashir, R., 2006. Characterization of vaccinia virus particles using microscale silicon cantilever resonators and atomic force microscopy. Sensors Actuators B Chem. 115, 189–197.
Kajzar, A., Cesa, C.M., Kirchgessner, N., Hoffmann, B., Merkel, R., 2008. Toward physiological conditions for cell analyses: forces of heart muscle cells suspended between elastic micropillars. Biophys. J. 94, 1854–1866.
Karabacak, N.M., Spuhler, P.S., Fachin, F., Lim, E.J., Pai, V., Ozkumur, E., et al., 2014. Microfluidic, marker-free isolation of circulating tumor cells from blood samples. Nat. Protoc. 9, 694–710.
Karlsson, R., 2004. SPR for molecular interaction analysis: a review of emerging application areas. J. Mol. Recognit. 17, 151–161.
Kim, D.R., Zheng, X., 2008. Numerical characterization and optimization of the microfluidics for nanowire biosensors. Nano Lett. 8, 3233–3237.
Kim, A., Ah, C.S., Yu, H.Y., Yang, J.H., Baek, I.B., Ahn, C.G., et al., 2007. Ultrasensitive, label-free, and real-time immunodetection using silicon field-effect transistors. Appl. Phys. Lett. 91.
Kotz, K.T., Xiao, W., Miller-Graziano, C., Qian, W.J., Russom, A., Warner, E.A., et al., 2010. Clinical microfluidics for neutrophil genomics and proteomics. Nat. Med. 16, 1042–1047.
Kraning-Rush, C.M., Califano, J.P., Reinhart-King, C.A., 2012. Cellular traction stresses increase with increasing metastatic potential. PLoS One 7, e32572.
Kshitiz, Park, J., Kim, P., Helen, W., Engler, A.J., Levchenko, A., et al., 2012. Control of stem cell fate and function by engineering physical microenvironments. Integr. Biol. 4, 1008–1018.
Kuo, C.W., Shiu, J.Y., Chien, F.C., Tsai, S.M., Chueh, D.Y., Chen, P., 2010. Polymeric nanopillar arrays for cell traction force measurements. Electrophoresis 31, 3152–3158.
Kuo, C.W., Chien, F.C., Shiu, J.Y., Tsai, S.M., Chueh, D.Y., Hsiao, Y.S., et al., 2011. Investigation of the growth of focal adhesions using protein nanoarrays fabricated by nanocontact printing using size tunable polymeric nanopillars. Nanotechnology 22, 265302.
Lai, J., Perazzo, T., Shi, Z., Majumdar, A., 1997. Optimization and performance of high-resolution micro-optomechanical thermal sensors. Sensors Actuators A Phys. 58, 113–119.
Leckband, D.E., Kuhl, T.L., Wang, H.K., Muller, W., Herron, J., Ringsdorf, H., 2000. Force probe measurements of antibody–antigen interactions. Methods 20, 329–340.
Lee, S.J., Park, J.S., Im, H.T., Jung, H.I., 2008a. A microfluidic ATP-bioluminescence sensor for the detection of airborne microbes. Sensors Actuators B Chem. 132, 443–448.
Lee, S.J., Youn, B.S., Park, J.W., Niazi, J.H., Kim, Y.S., Gu, M.B., 2008b. ssDNA aptamer-based surface plasmon resonance biosensor for the detection of retinol binding protein 4 for the early diagnosis of type 2 diabetes. Anal. Chem. 80, 2867–2873.
Lee, J., Icoz, K., Roberts, A., Ellington, A.D., Savran, C.A., 2010. Diffractometric detection of proteins using microbead-based rolling circle amplification. Anal. Chem. 82, 197–202.
Legant, W.R., Miller, J.S., Blakely, B.L., Cohen, D.M., Genin, G.M., Chen, C.S., 2010. Measurement of mechanical tractions exerted by cells in three-dimensional matrices. Nat. Methods 7, 969–971.
Lemmon, C.A., Sniadecki, N.J., Ruiz, S.A., Tan, J.L., Romer, L.H., Chen, C.S., 2005. Shear force at the cell–matrix interface: enhanced analysis for microfabricated post array detectors. Mech. Chem. Biosyst. 2, 1–16.
Li, J., Ng, H.T., Cassell, A., Fan, W., Chen, H., Ye, Q., et al., 2003. Carbon nanotube nanoelectrode array for ultrasensitive DNA detection. Nano Lett. 3, 597–602.
Li, C., Curreli, M., Lin, H., Lei, B., Ishikawa, F.N., Datar, R., et al., 2005. Complementary detection of prostate-specific antigen using In(2)O(3) nanowires and carbon nanotubes. J. Am. Chem. Soc. 127, 12484–12485.
Li, S.Q., Orona, L., Li, Z.M., Cheng, Z.Y., 2006. Biosensor based on magnetostrictive microcantilever. Appl. Phys. Lett. 88.
Li, L., Bennett, S.A., Wang, L., 2012. Role of E-cadherin and other cell adhesion molecules in survival and differentiation of human pluripotent stem cells. Cell Adhes. Migr. 6, 59–70.
Li, P., Mao, Z., Peng, Z., Zhou, L., Chen, Y., Huang, P.H., et al., 2015. Acoustic separation of circulating tumor cells. Proc. Natl. Acad. Sci. U. S. A. 112, 4970–4975.
Lin, H.K., Zheng, S., Williams, A.J., Balic, M., Groshen, S., Scher, H.I., et al., 2010. Portable filter-based microdevice for detection and characterization of circulating tumor cells. Clin. Cancer Res. 16, 5011–5018.
Lin, S.C., Mao, X., Huang, T.J., 2012. Surface acoustic wave (SAW) acoustophoresis: now and beyond. Lab Chip 12, 2766–2770.
Lowe, C.R., Hin, B.F.Y.Y., Cullen, D.C., Evans, S.E., Stephens, L.D.G., Maynard, P., 1990. Biosensors. J. Chromatogr. 510, 347–354.
Lu, Y., Liu, G.L., Lee, L.P., 2005. High-density silver nanoparticle film with temperature-controllable interparticle spacing for a tunable surface enhanced Raman scattering substrate. Nano Lett. 5, 5–9.
Maehashi, K., Katsura, T., Kerman, K., Takamura, Y., Matsumoto, K., Tamiya, E., 2007. Label-free protein biosensor based on aptamer-modified carbon nanotube field-effect transistors. Anal. Chem. 79, 782–787.
Maheshwari, G., Brown, G., Lauffenburger, D.A., Wells, A., Griffith, L.G., 2000. Cell adhesion and motility depend on nanoscale RGD clustering. J. Cell Sci. 113 (Pt 10), 1677–1686.
Makani, J., Cox, S.E., Soka, D., Komba, A.N., Oruo, J., Mwamtemi, H., et al., 2011. Mortality in sickle cell anemia in Africa: a prospective cohort study in Tanzania. PLoS One 6.
Manalis, S.R., Minne, S.C., Atalar, A., Quate, C.F., 1996. Interdigital cantilevers for atomic force microscopy. Appl. Phys. Lett. 69, 3944–3946.
Marelli, M., Gadhari, N., Boero, G., Chiquet, M., Brugger, J., 2014. Cell force measurements in 3D microfabricated environments based on compliant cantilevers. Lab Chip 14, 286–293.
McKendry, R., Zhang, J.Y., Arntz, Y., Strunz, T., Hegner, M., Lang, H.P., et al., 2002. Multiple label-free biodetection and quantitative DNA-binding assays on a nanomechanical cantilever array. Proc. Natl. Acad. Sci. U. S. A. 99, 9783–9788.
McNamara, L.E., McMurray, R.J., Biggs, M.J., Kantawong, F., Oreffo, R.O., Dalby, M.J., 2010. Nanotopographical control of stem cell differentiation. J. Tissue Eng. 2010, 120623.

Please cite this article as: Alapan, Y., et al., Micro- and nanodevices integrated with biomolecular probes, Biotechnol Adv (2015), http://dx.doi.org/10.1016/j.biotechadv.2015.09.001

Mehta, P., Cummings, R.D., McEver, R.P., 1998. Affinity and kinetic analysis of P-selectin binding to P-selectin glycoprotein ligand-1. J. Biol. Chem. 273, 32506–32513.
Meltzer, R.H., Krogmeier, J.R., Kwok, L.W., Allen, R., Crane, B., Griffis, J.W., et al., 2011. A lab-on-chip for biothreat detection using single-molecule DNA mapping. Lab Chip 11, 863–873.
Moon, S., Gurkan, U.A., Blander, J., Fawzi, W.W., Aboud, S., Mugusi, F., et al., 2011. Enumeration of CD4+ T-cells using a portable microchip count platform in Tanzanian HIV-infected patients. PLoS One 6, e21409.
Moore, D.F., Syms, R.R.A., 1999. Recent developments in micromachined silicon. Electron. Commun. Eng. 11, 261–270.
Murthy, S.K., Sin, A., Tompkins, R.G., Toner, M., 2004. Effect of flow and surface conditions on human lymphocyte isolation using microfluidic chambers. Langmuir 20, 11649–11655.
Nagrath, S., Sequist, L.V., Maheswaran, S., Bell, D.W., Irimia, D., Ulkus, L., et al., 2007. Isolation of rare circulating tumour cells in cancer patients by microchip technology. Nature 450, 1235–1239.
Nair, P.R., Alam, M.A., 2010. Theory of "selectivity" of label-free nanobiosensors: a geometro-physical perspective. J. Appl. Phys. 107, 64701.
Nam, J., Lim, H., Kim, D., Shin, S., 2011. Separation of platelets from whole blood using standing surface acoustic waves in a microchannel. Lab Chip 11, 3361–3364.
Nutiu, R., Li, Y., 2003. Structure-switching signaling aptamers. J. Am. Chem. Soc. 125, 4771–4778.
Ohk, S.H., Koo, O.K., Sen, T., Yamamoto, C.M., Bhunia, A.K., 2010. Antibody-aptamer functionalized fibre-optic biosensor for specific detection of *Listeria monocytogenes* from food. J. Appl. Microbiol. 109, 808–817.
Ohnaga, T., Shimada, Y., Moriyama, M., Kishi, H., Obata, T., Takata, K., et al., 2013. Polymeric microfluidic devices exhibiting sufficient capture of cancer cell line for isolation of circulating tumor cells. Biomed. Microdevices 15, 611–616.
Onaran, A.G., Balantekin, M., Lee, W., Hughes, W.L., Buchine, B.A., Guldiken, R.O., et al., 2006. A new atomic force microscope probe with force sensing integrated readout and active tip. Rev. Sci. Instrum. 77.
Ozkumur, E., Shah, A.M., Ciciliano, J.C., Emmink, B.L., Miyamoto, D.T., Brachtel, E., et al., 2013. Inertial focusing for tumor antigen-dependent and -independent sorting of rare circulating tumor cells. Sci. Transl. Med. 5, 179ra47.
Paddle, B.M., 1996. Biosensors for chemical and biological agents of defence interest. Biosens. Bioelectron. 11, 1079–1113.
Park, K., Jang, J., Irimia, D., Sturgis, J., Lee, J., Robinson, J.P., et al., 2008. 'Living cantilever arrays' for characterization of mass of single live cells in fluids. Lab Chip 8, 1034–1041.
Patolsky, F., Zheng, G.F., Hayden, O., Lakadamyali, M., Zhuang, X.W., Lieber, C.M., 2004. Electrical detection of single viruses. Proc. Natl. Acad. Sci. U. S. A. 101, 14017–14022.
Patolsky, F., Timko, B.P., Yu, G.H., Fang, Y., Greytak, A.B., Zheng, G.F., et al., 2006. Detection, stimulation, and inhibition of neuronal signals with high-density nanowire transistor arrays. Science 313, 1100–1104.
Pei, J.H., Tian, F., Thundat, T., 2004. Glucose biosensor based on the microcantilever. Anal. Chem. 76, 292–297.
Perroud, T.D., Kaiser, J.N., Sy, J.C., Lane, T.W., Branda, C.S., Singh, A.K., et al., 2008. Microfluidic-based cell sorting of *Francisella tularensis* infected macrophages using optical forces. Anal. Chem. 80, 6365–6372.
Pierce, K.L., Premont, R.T., Lefkowitz, R.J., 2002. Seven-transmembrane receptors. Nat. Rev. Mol. Cell Biol. 3, 639–650.
Plouffe, B.D., Kniazeva, T., Mayer Jr., J.E., Murthy, S.K., Sales, V.L., 2009. Development of microfluidics as endothelial progenitor cell capture technology for cardiovascular tissue engineering and diagnostic medicine. FASEB J. 23, 3309–3314.
Pommer, M.S., Zhang, Y., Keerthi, N., Chen, D., Thomson, J.A., Meinhart, C.D., et al., 2008. Dielectrophoretic separation of platelets from diluted whole blood in microfluidic channels. Electrophoresis 29, 1213–1218.
Rabodzey, A., Alcaide, P., Luscinskas, F.W., Ladoux, B., 2008. Mechanical forces induced by the transendothelial migration of human neutrophils. Biophys. J. 95, 1428–1438.
Raiteri, R., Grattarola, M., Butt, H.J., Skladal, P., 2001. Micromechanical cantilever-based biosensors. Sensors Actuators B Chem. 79, 115–126.
Rizvi, I., Gurkan, U.A., Tasoglu, S., Alagic, N., Celli, J.P., Mensah, L.B., et al., 2013. Flow induces epithelial–mesenchymal transition, cellular heterogeneity and biomarker modulation in 3D ovarian cancer nodules. Proc. Natl. Acad. Sci. U. S. A.
Saez, A., Ghibaudo, M., Buguin, A., Silberzan, P., Ladoux, B., 2007. Rigidity-driven growth and migration of epithelial cells on microstructured anisotropic substrates. Proc. Natl. Acad. Sci. U. S. A. 104, 8281–8286.
Savran, C.A., Sparks, A.W., Sihler, J., Li, J., Wu, W.C., Berlin, D.E., et al., 2002. Fabrication and characterization of a micromechanical sensor for differential detection of nanoscale motions. J. Microelectromech. Syst. 11, 703–708.
Savran, C.A., Knudsen, S.M., Ellington, A.D., Manalis, S.R., 2004. Micromechanical detection of proteins using aptamer-based receptor molecules. Anal. Chem. 76, 3194–3198.
Schmid, K., Rosa, E.C., Macnair, M.B., 1956. Fractionation of the proteins of human synovial fluid and plasma. J. Biol. Chem. 219, 769–780.
Shafiee, H., Asghar, W., Inci, F., Yuksekkaya, M., Jahangir, M., Zhang, M.H., et al., 2015. Paper and Flexible Substrates as Materials for Biosensing Platforms to Detect Multiple Biotargets. Sci. Rep. 5, 8719.
Shastri, A., McGregor, L.M., Liu, Y., Harris, V., Nan, H., Mujica, M., et al., 2015. An aptamer-functionalized chemomechanically modulated biomolecule catch-and-release system. Nat. Chem. 7, 447–454.
Sheng, W., Chen, T., Kamath, R., Xiong, X., Tan, W., Fan, Z.H., 2012. Aptamer-enabled efficient isolation of cancer cells from whole blood using a microfluidic device. Anal. Chem. 84, 4199–4206.
Sin, A., Murthy, S.K., Revzin, A., Tompkins, R.G., Toner, M., 2005. Enrichment using antibody-coated microfluidic chambers in shear flow: model mixtures of human lymphocytes. Biotechnol. Bioeng. 91, 816–826.
Singh, A., Suri, S., Lee, T., Chilton, J.M., Cooke, M.T., Chen, W., et al., 2013. Adhesion strength-based, label-free isolation of human pluripotent stem cells. Nat. Methods.
Sniadecki, N.J., Desai, R.A., Ruiz, S.A., Chen, C.S., 2006. Nanotechnology for cell–substrate interactions. Ann. Biomed. Eng. 34, 59–74.
Sniadecki, N.J., Anguelouch, A., Yang, M.T., Lamb, C.M., Liu, Z., Kirschner, S.B., et al., 2007. Magnetic microposts as an approach to apply forces to living cells. Proc. Natl. Acad. Sci. U. S. A. 104, 14553–14558.
So, H.M., Won, K., Kim, Y.H., Kim, B.K., Ryu, B.H., Na, P.S., et al., 2005. Single-walled carbon nanotube biosensors using aptamers as molecular recognition elements. J. Am. Chem. Soc. 127, 11906–11907.
Sone, H., Ikeuchi, A., Izumi, T., Okano, H., Hosaka, S., 2006. Femtogram mass biosensor using self-sensing cantilever for allergy check. Jpn. J. Appl. Phys. 45, 2301–2304 (1).
Springer, T.A., 1990. Adhesion receptors of the immune system. Nature 346, 425–434.
Staples, M., Daniel, K., Cima, M.J., Langer, R., 2006. Application of micro- and nano-electromechanical devices to drug delivery. Pharm. Res. 23, 847–863.
Stern, E., Klemic, J.F., Routenberg, D.A., Wyrembak, P.N., Turner-Evans, D.B., Hamilton, A.D., et al., 2007. Label-free immunodetection with CMOS-compatible semiconducting nanowires. Nature 445, 519–522.
Stoney, G.G., 1909. The tension of metallic films deposited by electrolysis. Proc. R. Soc. Lond. A 82, 172–175.
Storri, S., Santoni, T., Minunni, M., Mascini, M., 1998. Surface modifications for the development of piezoimmunosensors. Biosens. Bioelectron. 13, 347–357.
Stott, S.L., Hsu, C.H., Tsukrov, D.I., Yu, M., Miyamoto, D.T., Waltman, B.A., et al., 2010. Isolation of circulating tumor cells using a microvortex-generating herringbone-chip. Proc. Natl. Acad. Sci. U. S. A. 107, 18392–18397.
Sulchek, T., Hsieh, R., Minne, S.C., Quate, C.F., Manalis, S.R., 2001. Interdigital cantilever as a biological sensor. Proceedings of the 2001 1st IEEE Conference on Nanotechnology, pp. 562–566.
Suzuki, K., Takahashi, K., 2003. Reduced cell adhesion during mitosis by threonine phosphorylation of beta1 integrin. J. Cell. Physiol. 197, 297–305.
Tan, J.L., Tien, J., Pirone, D.M., Gray, D.S., Bhadriraju, K., Chen, C.S., 2003. Cells lying on a bed of microneedles: an approach to isolate mechanical force. Proc. Natl. Acad. Sci. U. S. A. 100, 1484–1489.
Tang, T., Liu, X.L., Li, C., Lei, B., Zhang, D.H., Rouhanizadeh, M., et al., 2005. Complementary response of In_2O_3 nanowires and carbon nanotubes to low-density lipoprotein chemical gating. Appl. Phys. Lett. 86.
Tasoglu, S., Gurkan, U.A., Wang, S., Demirci, U., 2013. Manipulating biological agents and cells in micro-scale volumes for applications in medicine. Chem. Soc. Rev. 42 (13), 5788–5808.
Ting, L.H., Jahn, J.R., Jung, J.I., Shuman, B.R., Feghhi, S., Han, S.J., et al., 2012. Flow mechanotransduction regulates traction forces, intercellular forces, and adherens junctions. Am. J. Physiol. Heart Circ. Physiol. 302, H2220–H2229.
Unal, M., Alapan, Y., Jia, H., Varga, A.G., Angelino, K., Aslan, M., Sayin, I., Han, C., Jiang, Y., Zhang, Z., Gurkan, U.A., 2014. Micro and nano-scale technologies for cell mechanics. Nanobiomedicine 1, 5. http://dx.doi.org/10.5772/59379.
Vermeulen, M., Le Pesteur, F., Gagnerault, M.C., Mary, J.Y., Sainteny, F., Lepault, F., 1998. Role of adhesion molecules in the homing and mobilization of murine hematopoietic stem and progenitor cells. Blood 92, 894–900.
Vickers, D.A., Chory, E.J., Murthy, S.K., 2012. Separation of two phenotypically similar cell types via a single common marker in microfluidic channels. Lab Chip 12, 3399–3407.
Wang, Y.K., Chen, C.S., 2013. Cell adhesion and mechanical stimulation in the regulation of mesenchymal stem cell differentiation. J. Cell. Mol. Med.
Wang, J.H., Li, B., 2009. Application of cell traction force microscopy for cell biology research. Methods Mol. Biol. 586, 301–313.
Wang, M.M., Tu, E., Raymond, D.E., Yang, J.M., Zhang, H., Hagen, N., et al., 2005. Microfluidic sorting of mammalian cells by optical force switching. Nat. Biotechnol. 23, 83–87.
Wang, X., Chen, S., Kong, M., Wang, Z., Costa, K.D., Li, R.A., et al., 2011. Enhanced cell sorting and manipulation with combined optical tweezer and microfluidic chip technologies. Lab Chip 11, 3656–3662.
Wang, S., Esfahani, M., Gurkan, U.A., Inci, F., Kuritzkes, D.R., Demirci, U., 2012. Efficient on-chip isolation of HIV subtypes. Lab Chip 12, 1508–1515.
Wang, S., Tasoglu, S., Chen, P.Z., Chen, M., Akbas, R., Wach, S., et al., 2014. Micro-a-fluidics ELISA for rapid CD4 cell count at the point-of-care. Sci. Rep. 4, 3796.
Watkins, N.N., Hassan, U., Damhorst, G., Ni, H., Vaid, A., Rodriguez, W., et al., 2013. Microfluidic CD4+ and CD8+ T lymphocyte counters for point-of-care HIV diagnostics using whole blood. Sci. Transl. Med. 5, 214ra170.
Weizmann, Y., Patolsky, F., Lioubashevski, O., Willner, I., 2004. Magneto-mechanical detection of nucleic acids and telomerase activity in cancer cells. J. Am. Chem. Soc. 126, 1073–1080.
Wu, G.H., Datar, R.H., Hansen, K.M., Thundat, T., Cote, R.J., Majumdar, A., 2001. Bioassay of prostate-specific antigen (PSA) using microcantilevers. Nat. Biotechnol. 19, 856–860.
Xu, T., Lu, B., Tai, Y.C., Goldkorn, A., 2010. A cancer detection platform which measures telomerase activity from live circulating tumor cells captured on a microfilter. Cancer Res. 70, 6420–6426.
Yang, M.T., Fu, J., Wang, Y.K., Desai, R.A., Chen, C.S., 2011. Assaying stem cell mechanobiology on microfabricated elastomeric substrates with geometrically modulated rigidity. Nat. Protoc. 6, 187–213.
Yaralioglu, G.G., Atalar, A., Manalis, S.R., Quate, C.F., 1998. Analysis and design of an interdigital cantilever as a displacement sensor. J. Appl. Phys. 83, 7405–7415.
Yoon, J.-Y., Garrell, R.L., 2014. Biomolecular adsorption in microfluidics. Encyclopedia of Microfluidics and Nanofluidics. Springer, pp. 1–13.

Please cite this article as: Alapan, Y., et al., Micro- and nanodevices integrated with biomolecular probes, Biotechnol Adv (2015), http://dx.doi.org/10.1016/j.biotechadv.2015.09.001

Yu, Z.T., Aw Yong, K.M., Fu, J., 2014. Microfluidic blood cell sorting: now and beyond. Small 10, 1687–1703.
Zeng, S., Baillargeat, D., Ho, H.P., Yong, K.T., 2014. Nanomaterials enhanced surface plasmon resonance for biological and chemical sensing applications. Chem. Soc. Rev. 43, 3426–3452.
Zhang, J., Lang, H.P., Huber, F., Bietsch, A., Grange, W., Certa, U., et al., 2006. Rapid and label-free nanomechanical detection of biomarker transcripts in human RNA. Nat. Nanotechnol. 1, 214–220.
Zhang, J., Sheng, W., Fan, Z.H., 2014. An ensemble of aptamers and antibodies for multivalent capture of cancer cells. Chem. Commun. (Camb.) 50, 6722–6725.

Please cite this article as: Alapan, Y., et al., Micro- and nanodevices integrated with biomolecular probes, Biotechnol Adv (2015), http://dx.doi.org/10.1016/j.biotechadv.2015.09.001